Passive Stiffness Characteristics of the Scoliotic Lumbar Torso in Trunk Flexion, Extension, Lateral Bending, and Axial Rotation

Steven Drew Voinier

Thesis submitted to the faculty of the Virginia Polytechnic Institute and State University in partial fulfillment of the requirements for the degree of

Master of Science

In

Mechanical Engineering

Michael J. Agnew, Co-Chair

Maury A. Nussbaum, Co-Chair

Thurmon E. Lockhart

February 20, 2015

Blacksburg, Virginia

Keywords: Scoliosis, Stiffness, Neutral Zone

Passive Stiffness Characteristics of the Scoliotic Lumbar Torso in Trunk Flexion, Extension, Lateral bending, and Axial Rotation

Steven Drew Voinier

ABSTRACT

As the average American age increases, there is a need to study the spine biomechanics of adults with scoliosis. Most studies examining the mechanics of scoliosis have focused on *in vitro* testing or computer simulations, but *in vivo* testing of the mechanical response of a scoliotic spine has not yet been reported. The purpose of this study was to quantitatively define the passive stiffness properties of the *in vivo* scoliotic spine in three principle anatomical motions and identify differences relative to healthy controls.

Scoliotic (n=14) and control (n=17) participants with no history of spondylolisthesis, spinal fracture, or spinal surgery participated in three different tests (torso lateral side bending, torso axial rotation, and torso flexion/extension) that isolated mobility to the *in vivo* lumbar spine. Scoliotic individuals with Cobb angles ranging 15-75 degrees were accepted. Applied torque was measured using a uni-directional load cell, and inertial measurement units (IMU) recorded angular displacement of the upper torso relative to the pelvis and lower extremities. Torque-rotational displacement data were fit using a double sigmoid function, resulting in excellent overall fit ($R^2 > 0.901$). The neutral zone (NZ) width, or the range of motion where there is minimal internal resistance, was then calculated. Stiffnesses within the NZ and outside of the NZ were also calculated. Stiffness asymmetries were also computed within each trial. These parameters were statistically compared between factor of population and within factor of direction.

There was an interaction effect between populations when comparing axial twist NZ width and lateral bend NZ width. The lateral bend NZ width magnitude was significantly smaller in scoliotic patients. NZ stiffness in the all three directions was greater in the scoliotic population. There was no significant difference in asymmetrical stiffness between populations.

The present study is the first investigation to quantify the *in vivo* neutral zone and related mechanics of the scoliotic lumbar spine. Future research is needed to determine if the measured lumbar spine mechanical characteristics can help explain progression of scoliosis and complement scoliosis classification systems.

Acknowledgements

To my advisor, Dr. Michael Agnew, thank you for supporting my interest in scoliosis research and providing a simple, yet intuitive approach to analysis the mechanics of scoliosis. I was able to gain valuable knowledge through this research project. Being the only graduate student on this project, your hands on approach and patience allowed me to complete this thesis. To my co-chair, Dr. Nussbaum, thank you for appropriately questioning my methods and hypothesizes in order for me to ask and answer the right questions. To Dr. Lockhart, thank you for noticing my enthusiasm for the scoliosis and pushing me to pursue a research examining the disease. To Dr. Jonathan Carmouche, thank you for collaborating with me on this project and providing me with scoliosis patients. I also appreciate the free burrito after that long day.

To Ralph Cullen, thank you for explaining the complicated LabView data acquisition code and providing suggestions to improve my project. To Peter Fino, thank you for helping me through the process of attaining this degree and staying late to help pack the equipment. To Nora Fino, thank you for imparting your extensive knowledge of statistics onto me. To Christopher Frames, thank you for letting me borrow your car on short notice and providing your muscle to load and unload the equipment over and over again. To Randy Waldron, thank you for working with me to quickly fabricate my testing apparatus.

To my parents, thank you for your continued support not only with my master's degree, but with all of my dreams that I have pursued. The push is much appreciated. To Dana, thank you for all of the craziness that you had to deal with and still managing to stick with me.

TABLE OF CONTENTS

LIST OF FIGURES

LIST OF TABLES

1. INTRODUCTION

1.1. Rationale

Literature concerning adult scoliosis diagnosis and classification has been scarce until recently (Grubb, Lipscomb et al. 1988, Grubb and Lipscomb 1992, Schwab, el-Fegoun et al. 2005, Marty-Poumarat, Scattin et al. 2007, Grivas 2010), limiting the available knowledge doctors and engineers can use to mitigate or eliminate this spinal deformity. In a survey documenting the treatment of non-operative adult scoliosis, the total costs averaged over $10,000 per patient even though no general improvement in health status was observed (Glassman, Carreon et al. 2010). Another analysis found that scoliosis patients spent an average of $47,127 on surgical treatment, with implants contributing the most to overall cost (Ialenti, Lonner et al. 2010).

The prevalence of adult scoliosis ranges from 1-10% (Schwab, Smith et al. 2002, Kobayashi, Atsuta et al. 2006, Ploumis, Transfledt et al. 2007). Pain is one the most significant complaints reported by adult scoliosis patients (Grubb and Lipscomb 1992, Aebi 2005, Marty-Poumarat, Scattin et al. 2007, Grivas 2010, O'Brien 2010). In addition, back pain can be accompanied by radicular pain or claudication symptoms caused by localized compression or root traction. Because of imbalanced spine loading, overloaded and stressed paravertebral back muscles may also fatigue and consequently contribute to asymmetric loading of the spine (Jackson, Simmons et al. 1983, Aebi 2005). Meta-analyses have suggested that most if not all patients with degenerative onset scoliosis predominantly complain of stenosis symptoms, with 44% of the patients exhibiting mechanical back pain (Grubb and Lipscomb 1992). Other possible side effects of scoliosis include breathing limitations, decreased functionality, abnormal physical appearance, and lower perception of life quality (O'Brien 2010).

While adult scoliosis remains as a major health concern, major corrective surgery has been considered too risky due to the age and disease progression within these patients (Aebi 2005). Besides age, the care procedure for those with scoliosis is also influenced by timing decisions, effectiveness, costs, and possible surgical complications. Even though surgery is meant to restore the geometrical properties of the spine or stop progression, many problems can arise from the operation, including an altered stress and strain distribution on the un-fused vertebrae (Weiss and Goodall 2008). Also, there is a possibility of development of new deformities in the other anatomical planes of motion. Furthermore, some scoliotic curves can continue to progress after surgery due to failure of instrumentation and implants, which may warrant salvage and reconstructive surgery. Over 50% of treated patients experience a failure of surgical spinal fusion (Weiss and Goodall 2008). Other outcomes of the corrective surgery include post-operative back pain, possible infections, and adjacent disc disease (Grivas 2010).

The degree of adult scoliosis progression is a primary factor doctors use to determine the course of treatment. The occurrence of scoliosis modifies the elastic properties of the spine system and induces a new model of stress distribution leading to new elasto-plastic deformations of the supporting spine structures (Lupparelli, Pola et al. 2002). Once scoliosis begins, the asymmetric degeneration of the disc and facet joints also leads to asymmetric loading of the spinal area (Aebi 2005). This further contributes to the asymmetric loading of the intervertebral disc and progresses the curve. These changes in mechanics can result in mechanical instability among the curve's vertebral segments. A variety of indicators have been developed to determine the rate and severity of lumbar degenerative scoliosis progression including unilateral disc narrowing, osteophyte growth, and apical vertebral rotation (Kobayashi, Atsuta et al. 2006, Kohno, Ikeuchi et al. 2011, Seo, Ha et al. 2011). However, these indicators may have missed

some other factors that can predict adult scoliosis progression, specifically the resilience of the lumbar spine in different loading directions. Indicators from literature only describe the result of scoliosis progression, but do not specify a mechanical causation. This research study may provide insight into a mechanical indictor to predict the potential progression of scoliosis before the curve begins to worsen. Biomechanical properties defined in this research study could be used in early interventions of the disease and precautionary methods could mitigate the deformity severity.

The goal of this research was to better understand and quantify the basic mechanics of the adult scoliosis in hopes that these data may be employed in future therapy or surgery decisions. As the proportion of adults to children is increasing, adult scoliosis will present itself as a more frequent problem as compared with adolescent scoliosis (Chamie 2002, Aebi 2005). The adult scoliosis problem will become more evident as the adult-children ratio is projected to be doubled by year 2050 (Chamie 2002).

Specifically, this research quantified the stiffness characteristics of an adult scoliosis patient in flexion/extension, lateral, and axial ranges of motion. While *in vitro* testing has been studied along with computer simulations, a holistic approach to determine scoliotic trunk stiffness has not yet been tested. Scoliotic patients were tested on an apparatus that only allows for trunk rotation about the lumbar region of the spine. The angular displacement related to the force applied was utilized to compute stiffness and additional tissue parameters. These parameters were compared with a healthy population to determine the degree in which the presence of scoliosis changes the *in vivo* biomechanical properties of the lumbar spine.

1.2. Specific Aims

The purpose of this study was to qualitatively understand the passive stiffness properties of the scoliotic spine across three anatomical planes. A comparison against a healthy population was also needed to determine if the passive stiffness has been compromised or if the body has compensated for the physiological differences. This leads into the first specific aim of the study:

SPECIFIC AIM 1: Determine and quantify how the presence of adult degenerative lumbar scoliosis corresponds to differences in the stiffness properties of the lumbar spine, specifically in comparison to a healthy cohort in the three anatomical planes of motion.

A variety of studies in scoliosis physiology imply increased stiffness as compared to the healthy spine, specifically due to an increase of muscle fiber stiffness(Friden and Lieber 2003, Brown, Gregory et al. 2011).This leads to the first hypothesis:

HYPOTHESIS: Stiffness magnitudes of the scoliotic spine would increase with the presence of the spinal deformity in each anatomical direction.

SPECIFIC AIM 2: Define and contrast the biomechanical neutral zone (NZ) of the scoliotic spine in regards to healthy normal across three anatomical planes of motion.

The "neutral zone" is designated as the region of high laxity, or low stiffness magnitude, around a neutral position (Panjabi 1992). Within healthy normals, the neutral zone (NZ) is located around the resting anatomical position of the spine and is further defined by the passive characteristics of the spinal tissues. However, supporting structures of the scoliotic spine (e.g. intervertebral discs and spinal ligaments) may be asymmetrically altered across the sagittal, lateral, and transverse planes. The measurement of the NZ may provide insight into progression

of scoliosis as studies have shown NZ increases with disc degeneration (Panjabi 1992, Mimura, Panjabi et al. 1994). This mechanical alteration could lead to an increase as well as a location shift of the NZ. This concept leads to the second hypothesis:

HYPOTHESIS: The magnitude of the spinal neutral zone is increased in the scoliotic spine as compared to a healthy normal due to probable degeneration of intervertebral discs.

SPECIFIC AIM 3: Determine if stiffness properties of the scoliotic spine exhibit asymmetrical stiffness characteristics with right/left lateral bending and clockwise/counterclockwise axial twist.

Along with the possible asymmetrical NZ, the stiffness magnitudes may also be altered when comparing right/left lateral bending and clockwise/counterclockwise axial rotation. Since the deformed spine is already deviated from its healthy position, asymmetrically degenerated intervertebral discs, stretched spinal ligaments, and physiologically altered muscle could increase/decrease the stiffness characteristics unilaterally (Panjabi, Goel et al. 1982, Shafaq, Suzuki et al. 2012). The proposed bilateral asymmetric mechanics of the lumbar spine leads to the final hypothesis:

HYPOTHESIS: The scoliotic lumbar spine exhibits asymmetrical stiffness characteristics in the transverse and lateral planes of motion.

1.3. Implications

Presently, researchers have used *in vitro* methods or animal models to investigate the mechanics of the scoliotic spine (Waters and Morris 1973, Stokes, McBride et al. 2011, Shafaq, Suzuki et al. 2012). From these tests, stiffness characteristics of the spinal ligaments, intervertebral discs, and muscles have been be integrated into finite element models to simulate kinematics and kinetics of the spine (Ruberté, Natarajan et al. 2009, Moramarco, Pérez del Palomar et al. 2010). However, the simulated mechanical behavior of a spinal unit is not entirely reliable because research on *in vitro* spinal ligament stiffness magnitude and rate change of stiffness differ within the literature.(Zander, Rohlmann et al. 2004). For example, discrepancies arise even if non-linear vs linearized stiffness parameters are used for finite element modeling due to material property assumptions of ligamentous and intervertebral disc degenerations (Eberlein, Holzapfel et al. 2004). Still, researchers have employed numerical methods to determine the mechanics of the scoliotic spine (Lafage, Leborgne et al. 2002, Zander, Rohlmann et al. 2004, Little and Adam 2009, Lafon, Lafage et al. 2010). To the authors' knowledge, these methods have not been verified by any *in vivo* experimental data. These definitions of *in vivo* mechanical characteristics of the scoliotic spine may ultimately improve spine models to help doctors and engineers predict the outcomes of scoliotic surgery (Petit, Aubin et al. 2004).

Furthermore, classification systems for adult scoliosis are necessary and frequently employed to properly diagnose and treat patients. The results of proposed study and methodology may contribute to and compliment these methodologies in tracking the progression of scoliosis, in addition to providing preliminary stiffness matrix data for other computational methods based on input parameters, such as geometry and magnitude of scoliosis.

2. LITERATURE REVIEW

Adult degenerative scoliosis is the asymmetric degeneration of discs and/or facet joints, leading to an asymmetric loading of the spinal segments. The scoliotic curve continues to progress as the deformity encourages the asymmetric loading on the discs. The progression of the curve can also deteriorate facet joints, joint capsules, and ligaments. The following sections will describe what the physiological changes are as a result of scoliosis and how experts classify scoliosis due to these changes. After, a review of spinal testing will be presented, including the definition of the neutral zone.

2.1. Biomechanical Definitions

Defining the mechanics of scoliosis requires introductory information concerning anatomical planes and mechanical characteristics of scoliosis.

Figure 2.1 depicts the anatomical planes of motion of the human body. The sagittal plane bisects the left and right side of the human body and flexion/extension movements occur in this plane. The coronal, or frontal, plane separates the anterior and posterior parts of the human body and lateral movements occur in this plane. The transverse plane separates the superior and inferior parts of the human body and axial movements occur in this plane.

Scoliotic patients exhibit significant spinal deformity in the coronal plane. The deformity severity can be quantified with the Cobb angle method. To measure the Cobb angle, the two vertebrae defining the upper and lower limits of the curve in the frontal plane must be defined. The angle between the end plate of the superior vertebrae and the end plate of the inferior vertebrae can be considered the Cobb angle (Cobb 1948). An exemplar Cobb angle is displayed in Figure 2.2. Adults exhibiting over a 10^{o} Cobb angle in the coronal plane can be considered scoliotic (Aebi 2005).

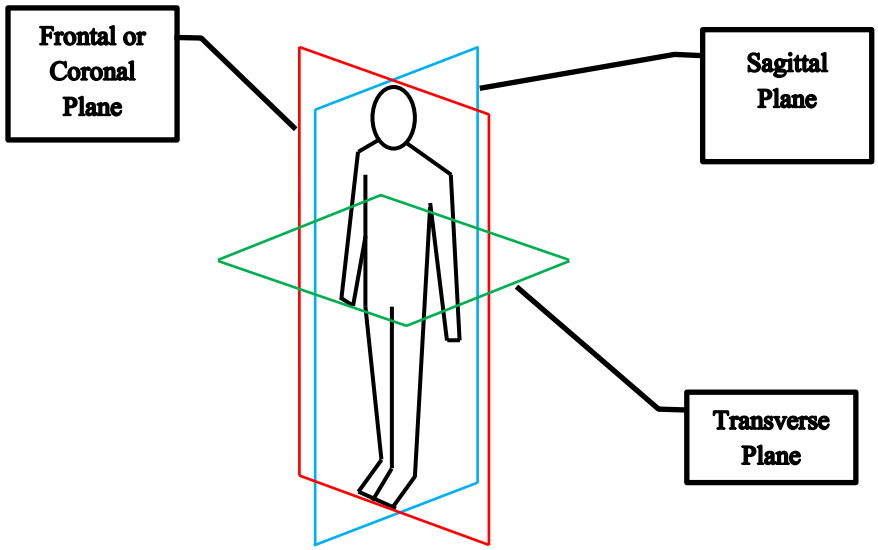

Figure 2.1 The anatomical planes of the human body

The destructive progression of scoliosis may additionally cause the body to show symptoms of spondylolisthesis, spondylarthritis, spondylosis, and spinal stenosis (Aebi 2005). A patient displays spondylolisthesis when adjacent vertebrae dislocate in the sagittal plane, resulting in an unstable joint. The body will react to this instability by forming osteophytes, or bone spurs, on the different parts of the vertebrae, which is classified as spondylarthritis or spondylosis. The buildup of osteophytes can also narrow the spinal canal, leading to spinal stenosis.

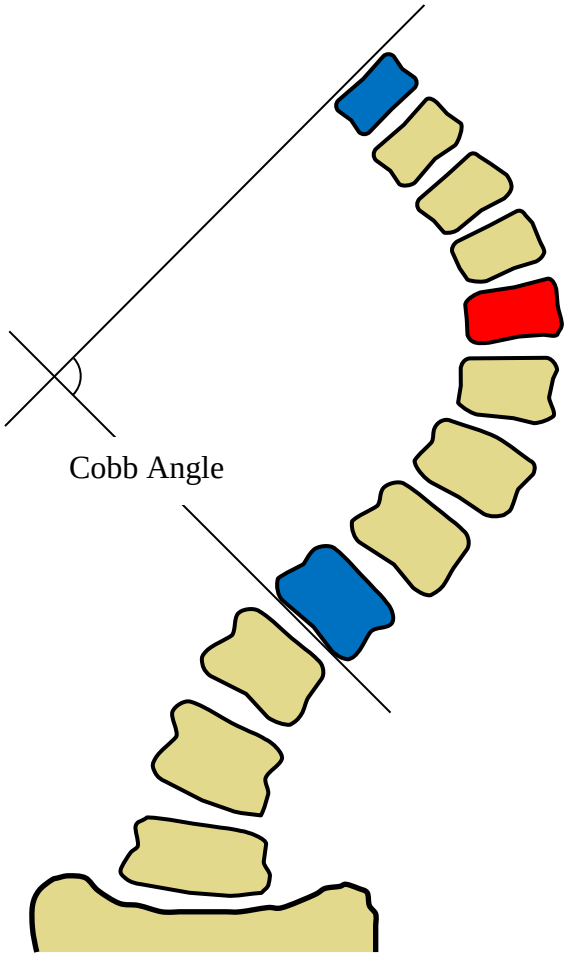

Figure 2.2 A measurement of the Cobb angle at the extreme ends of the curve. The blue vertebrae represent the limits of scoliotic curve. The red vertebrae represent the apex.

2.2. Physiological Changes

The passive stiffness of the spine depend on a variety of factors, including vertebral geometry, facet articulations, intervertebral discs, spinal ligaments, joint capsules, mechanical properties of muscles, and the skin (McGill, Seguin et al. 1994). As many features that affect spinal stiffness (e.g. ligaments, intervertebral discs, paraspinal musculature) are known to be altered in the scoliotic patient, it is reasonable to expect those who suffer from this condition to exhibit altered trunk stiffness with respect to a healthy individual. Furthermore, the asymmetries of the scoliotic spine may result in direction specific changes in passive, specifically right/left

lateral flexion and clockwise/counterclockwise rotation about the coronal and transverse planes, respectively. The following sections review literature on the physiological changes and symptoms in the scoliotic spine that could affect the overall trunk stiffness.

2.2.1. Spine Biomechanics

The spinal column is comprised of a series of bones called vertebrae. Typically, a vertebrae is comprised of an anterior body and a posterior vertebral arch (Gray 1918). The noteworthy portions of the vertebral arch are the spinous process, articular processes, and the transverse processes. The spinous process projected posteriorly while the two transverse processes project laterally from the vertebrae. Both the processes act an attachment points for ligaments and muscles. Two articular processes project superiorly and two articular processes project anteriorly. The surfaces are coated with cartilage and act as joint between adjacent vertebrae. A lumbar vertebra is displayed in Figure 2.3

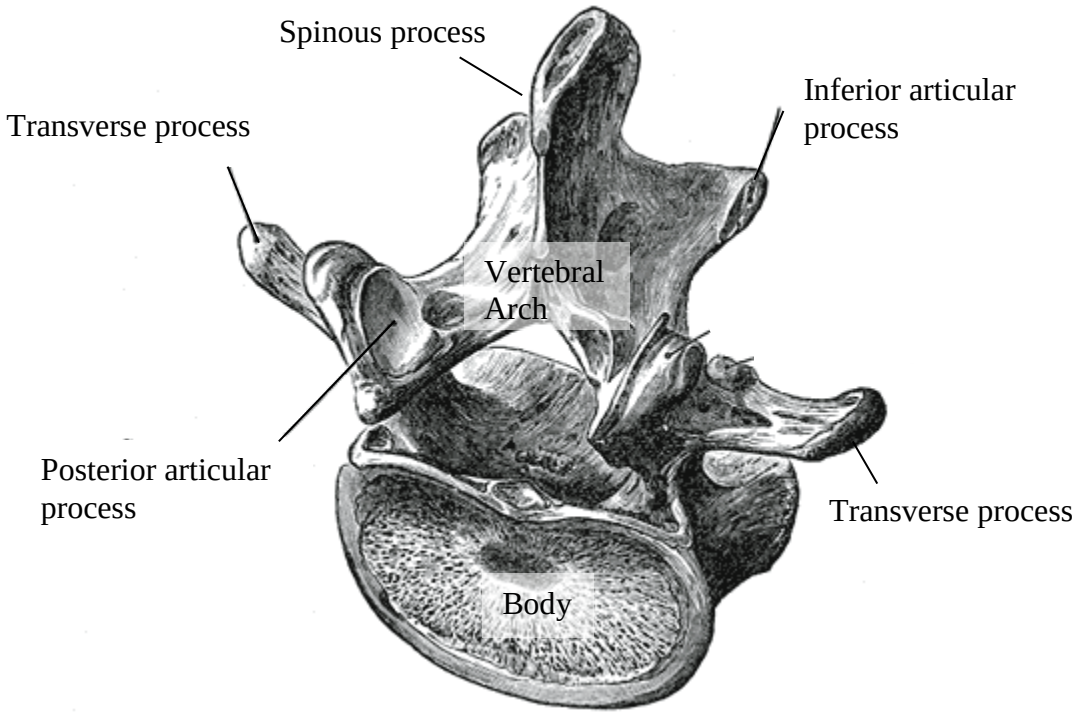

Figure 2.3 An isometric view of a lumbar vertebra. Gray, H. (1918). Anatomy of the Human Body. Philadelphia, Lea & Febiger. [public domain]

Spine movement involves complex kinematics and dynamics to achieve a desired motion. Because the spine is comprised of natural lordodic and kyphotic curves, flexion/extension and lateral bending of the torso also cause the vertebrae to rotate axially in a local reference frame (Veldhuizen and Scholten 1987). With scoliosis, the spinous processes are rotated towards the concave portion of the curve. Lateral flexion towards the concave portion will cause an increase in the Cobb angle while the lateral bending towards the convex side will decrease the Cobb angle. Furthermore, a numerical study illustrated the limited rotational coupled action during flexion/extension and lateral bending movements of a healthy spine (Lafage, Leborgne et al. 2002). In contrast, scoliotic spines evidenced considerable rotational coupled motion for the same motion simulations. However, other research has shown that a normal coupled movement between lateral bend and axial twist is present in healthy spines, but is not as apparent in scoliotic individuals (Beuerlein, Raso et al. 2003). As such, the geometrical alternations between a healthy and scoliotic spine can induce different forces within the spine, changing the stiffness characteristics of the spine as well.

The altered geometry of the scoliotic spine produces a stress distribution across an area that differs from a healthy spine (Lupparelli, Pola et al. 2002). As such, the altered elastic behavior of the spine and concentrated tensions create elasto-plastic deformation of the passive system. This geometric deformity can worsen over time based on the skeletal maturity level and the progressive elastic deformation of the passive restraining structures. Therefore, the restraining reactive forces are abnormally manipulated, consequently modifying the 3-dimensional kinematics of the motion segments. Furthermore, both age of the patient and the

location of the scoliosis can vary the strain and force distribution response from induced loads and/or physical demands.

The spinal passive structures do not provide significant stability in the neutral anatomical position. As a result, the active system (stabilizing muscles) must provide the mechanical integrity. Degradation of the active and the passive spinal system has been hypothesized to cause the neural system to overcompensate to restore spinal stability (Panjabi 1992). This may lead to detrimental changes including accelerated degeneration of spinal structures, muscle spasms, injury, and muscle fatigue. A degenerative disease like scoliosis may limit the load-bearing and stabilizing capability of the passive system.

2.2.2. Muscle

Posterior muscles of the trunk extend the vertebral column or stabilize the spinal column and keep it upright. Muscles along the length of the spinal column attach to the vertebral processes and ribs to produce movement. The serratus posterior inferior inserts at the spinous processes of the lower two thoracic and upper two lumbar vertebrae (Gray 1918). It branches at a laterally and superiorly and attaches on the lower four ribs.

The deeper muscles attaching to the lumbar spine include the sacrospinalis (erector spine), multifidus, interspinales, and the intertransversarii (Gray 1918), which can be found in Figure 2.4. The sacrospinalis ranges from the sacrum to the cervical spine. In the lumbar region, the scrospinalis is larger and divides into three regions: the lateral iliocostalis lumborum, the intermediate longissimus dorsi, and the medial spinalis dorsi. Located deeper to the sacrospinalis muscles is the multifidus muscle that also ranges the entire spinal column. The interspinales are short muscle pairs placed between the spinous processes of each adjacent vertebra. The intertransversarii are similar to the interspinales, but instead the muscles are placed between the transverse processes of each adjacent vertebra.

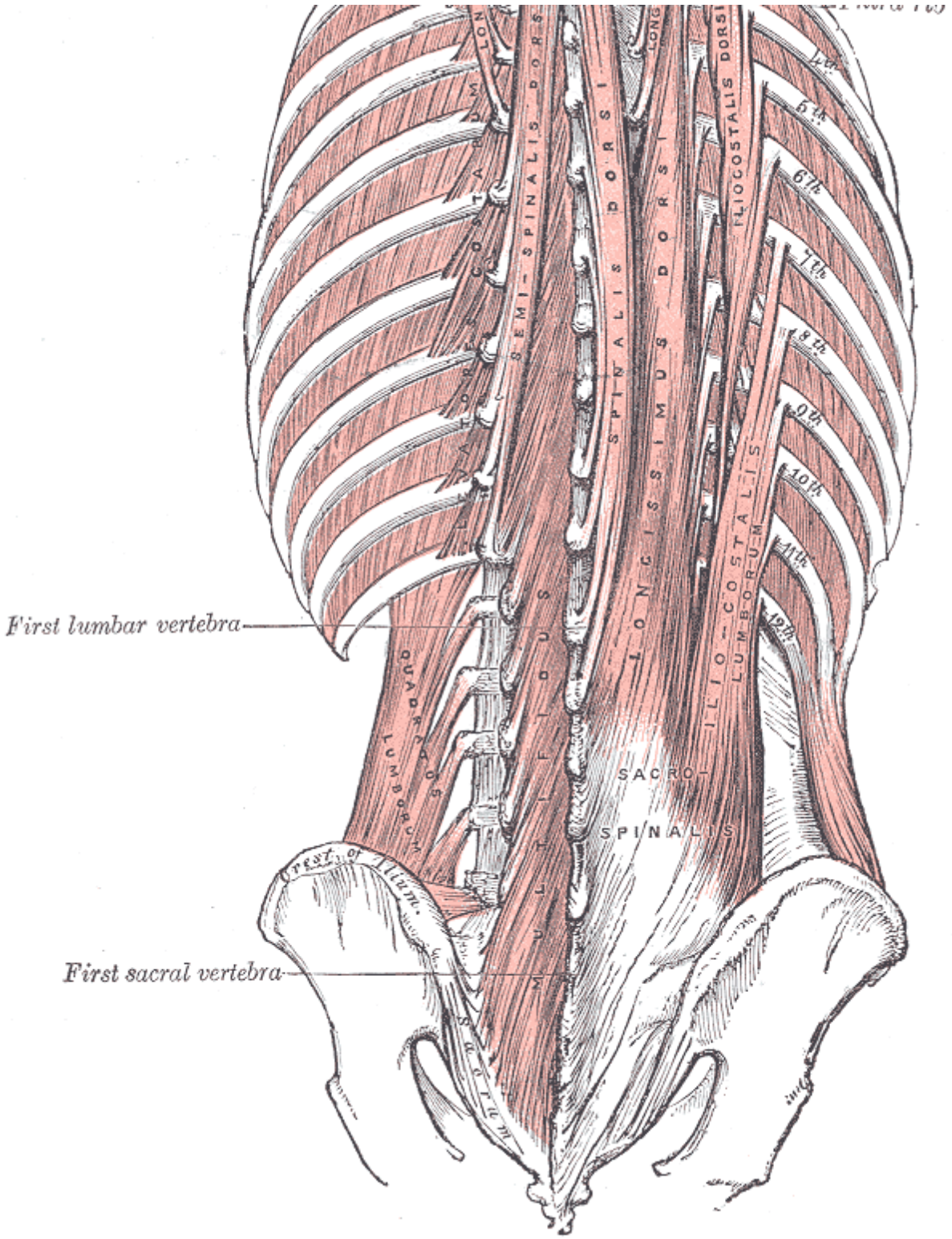

Figure 2.4 The deeper muscles of the spine. Gray, H. (1918). Anatomy of the Human Body. Philadelphia, Lea & Febiger. [public domain]

The posterior muscles of the abdomen, the quadratus lumborum, psoas major, and psoas minor, also attach the lumbar vertebrae (Gray 1918). The quadratus lumborum is located lateral and anterior to the sacrospinals in the lumbar section, as illustrated in Figure 2.5. It is inserted into the lower border of the last rib and the transverse processes of the upper four lumbar vertebrae. The other end of the muscle is attached to the upper crest of the pelvis bone. Both the psoas major and psoas minor at located anterior to both the quadratus lumborum and sacrospinalis muscles, displayed in Figure 2.5. The psoas major arises from the anterior portion of all the lumbar vertebrae transverse processes. It inserts to the top portion of the femur bone. The psoas minor, located anterior to the posas major, arises from the twelfth thoracic and the first lumbar vertebrae and is inserted into an anterior portion of the pelvis.

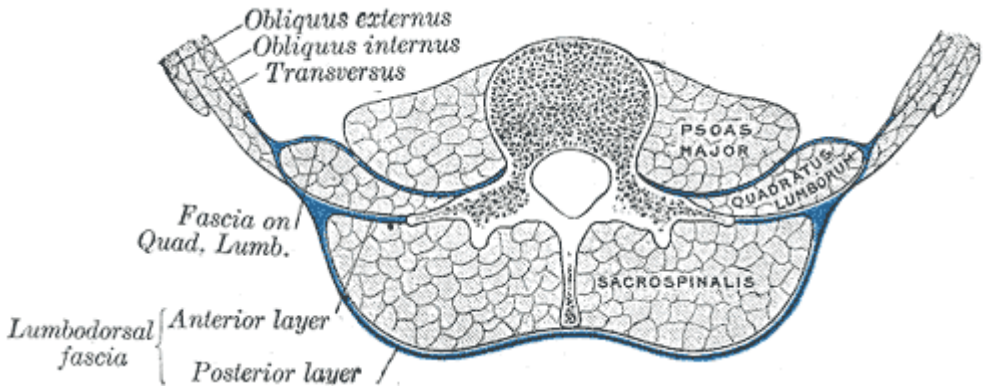

Figure 2.5 A top view of the muscles attached to the lumbar vertebrae. Gray, H. (1918). Anatomy of the Human Body. Philadelphia, Lea & Febiger. [public domain]

Indications of asymmetrical stiffness include muscular adaptions to the deformity. A study had shown that the paravertebral muscles and psoas of lumbar degenerative scoliotic patients exhibited asymmetrical muscle cross sectional area (CSA) (Kim, Lee et al. 2013). According to the authors, muscles located closer to the scoliotic spine on the convex side displayed a larger CSA as compared with the concave side irrespective to age, sex, and the direction and magnitude of the scoliotic apex. An asymmetrical physiological CSA could

indicate an increase of muscle fibers, leading to a resultant asymmetrical stiffness across the sagittal plane. The authors found that the quadratus lumborum muscle on the convex side is smaller than the concave side. However, the psoas major and multifidus muscles were larger on the convex side. The quadratus lumborum and other muscles located far from the spinal axis will be affected more by the deformity as compared to the paraspinal muscles located closer to the spine. The authors theorized that increased CSA of the psoas and multifidus muscles can be attributed to hypertrophy to compensate for the scoliotic curve. This theory may significantly change the torso stiffness depending on the anatomical movement. For example, the quadratus lumborum located laterally to spinal column may contribute to lateral bending stiffness more than extension. The psoas major, located anteriorly to spinal column, may have an opposite effect of the quadratus lumborum. This probable degeneration of spinal musculature is also coupled an observed higher percent fatty infiltration rate (% FIA) and smaller fiber diameter on the concave side compared to the convex side of the lumbar spine (Shafaq, Suzuki et al. 2012). The differences in material properties may also lead to differences in stiffness characteristics.

Because of disc degeneration in adult scoliosis, the passive mechanical properties of the supporting musculature may be affected (Brown, Gregory et al. 2011). With induced disc degeneration in rabbit subjects, stiffnesses of multifidus fiber bundles and individual fibers increased 107% and 34%, respectively. The stiffening occurred in muscles caudal to the degenerated disc site and would even extend at least two vertebral levels. As such, it is reasonable to expect that a scoliotic patient with disc degeneration might exhibit greater passive stiffness

Overstressed and fatigued lumbar paravertebral muscles in scoliotic patients may cause protective spasms. Friden and Lieber (2003) found that spastic fiber segments develop passive

tension at shorter sarcomere lengths as compared to normal fibers. This may support the finding of increased muscle fiber stiffness as reported in Brown, Gregory et al. (2011). In the Friden and Lieber study, the tangent modulus of the sarcomere length-stress relationship of the spastic fibers was approximately double in magnitude when compared to the studied normal fibers. Also, the length stress relationship of the spastic fibers was generally non-linear (20% of fibers were linear) as compared to the normal fibers (58% of fibers were linear), which may indicate that scoliotic patients may exhibit different stiffness characteristics in addition to increased stiffness. Another study discovered a reduction in type I fibers and an increase of type II fibers on the concave side of the scoliotic apex (Mannion, Meier et al. 1998). This may also affect the stiffness of a scoliotic individual since researchers have found differences in passive tension properties between fast and slow twitch muscle fibers (Prado, Makarenko et al. 2005).

2.2.3. Intervertebral Discs

The stability and mechanical integrity of connective tissues, like intervertebral discs and spinal ligaments, depend on the structural changes in the spinal system. The disc is composed of a collagen based annulus and nucleus filled with a proteoglycan gel to allow the spine to safely support compressive and torsional loads. Literature has stated that individual intervertebral disc exhibits stiffness quantities of 1.4-2.2Nm/^{o} in flexion, 2.0-2.8 Nm/^{o} for extension, 1.8-2.0 Nm/^{o} for lateral bending and 5 Nm/^{o} for axial torsion (Kurutz 2010). Zirbel, Stolworthy et al. (2013) examined the effect of degeneration on the axial twist, lateral bend, and flexion/extension stiffness characteristics. The authors found that lower levels of degeneration tended to reduce the stiffness of the disc while higher levels of degeneration lead to increased stiffness. The level of intervertebral disc degeneration in scoliotic patients may affect the observed *in vivo* stiffness.

The stability and mechanical integrity of connective tissues such as intervertebral discs depend on the degree and type of cross-links between the collagen fibers. The breakdown of

these fibers in degenerative cases will lead to a decreased resistance to movement. However, with increased degeneration, the vertical disc space is actually reduced, causing an increase in stiffness (Zirbel, Stolworthy et al. 2013). Concerning scoliosis, Duance, Crean et al. (1998) found that the convex portion of a scoliotic curve contains elevated levels of reducible cross-links as compared to the concave side of the curve. Also, inducing scoliosis in rat tails allowed the vertebrae to increase bending lateral stiffness as there was evidence of collagen remodeling to acclimate for the a scoliotic spinal position (Stokes, McBride et al. 2008, Stokes, McBride et al. 2011). Because the quantity of crosslinks between collagen relates to the stiffness of the disc, the asymmetrical collagen crosslink modeling may also be present in the asymmetrical stiffness characteristics proposed in this study.

2.2.4. Ligaments and Facet Joints

Ligaments provide significant reactive forces near the end range of motion to keep the spine aligned when vertebrae deviate from the neutral position. The six ligaments providing stiffness to the spine include the anterior longitudinal ligament (ALL), posterial longitudinal ligament (PLL), ligament flavum (LF), joint capsule (JC) of the zygapophyseal (facet) joint, intertransverse ligament (IL), interspinous ligament (ISL), and the supraspinous ligament (SSL). A sectioned view of the healthy spine is displayed in Figure 2.6, which depicts the placement of the spinal ligaments. The JC yields the highest stiffness characteristics, followed by the ALL, LF, SSL, PLL, and the ISL (Pintar, Yoganandan et al. 1992). The force deformation curves display similar tendencies for different levels of the spine from T12 to S1. When analyzing joint stiffness with a finite element model, ligaments displayed a strongly non-linear behavior with low stiffness and low strains (Zander, Rohlmann et al. 2004).

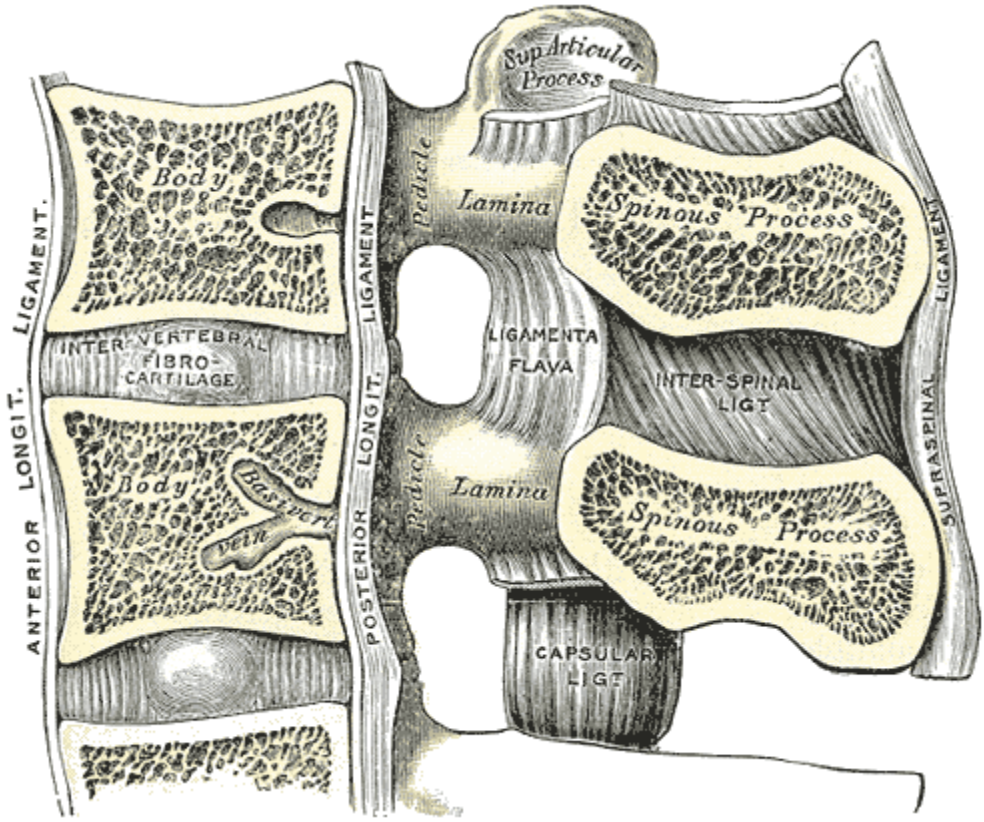

Figure 2.6 The sagittal plane section of the lumbar spine anatomy including ligaments and intervertebral discs. Gray, H. (1918). Anatomy of the Human Body. Philadelphia, Lea & Febiger. [public domain]

With a scoliotic spine in lateral flexion, Veldhuizen and Scholten (1987) proposed that asymmetrical displacements within the facet joints and asymmetrical tension within the spinal ligaments cause an alternative coupled movement of the scoliotic vertebral body as compared to a healthy vertebral body. Also, the mechanical strength of spinal ligaments decreases with age and facet joint degeneration (Iida, Abumi et al. 2002). Asymmetrical facet joint degeneration is also apparent in the scoliotic spine (Aebi 2005). This may alter the mechanics of the spine since research has shown facets supported no load in flexion, large loads during extension, torsion, and lateral bending (Schendel, Wood et al. 1993). A numerical study has identified that facet joints play an important role in the coupled movements of the spine due to contact reaction forces at articular surfaces (Shirazi-Adl 1994). A highly degenerated facet joint can result in a less

effective facet for coupling motion. Panjabi, Goel et al. (1982) examined the ligamentous strains in the normal spine for axial rotation, lateral bending, and flexion and extension. In flexion, the highest strains were present in the SSL and ISL ligaments. IL exhibited the highest strain in lateral bending, followed by LF, and JC. Rotation caused the highest strains in the JC while the remainder of the ligaments did not offer much resistance. The author also noted that axial range of motion was significantly larger for degenerated case as compared to a healthy spine, but smaller in the lateral bending and flexion. The author also predicted there is a higher probability of over-stretched ligaments in a degenerated spine since the neutral zone is generally wider for degenerated spines. This same phenomenon may also be evident in the proposed study since subjects will have degenerated lumbar spines.

2.3. Adult Scoliosis Classification

Because the concern for adult scoliosis has arisen only recently, classification systems are still being constructed to determine what method of treatment should ultimately be taken. The following sections will describe the parameters that define classification systems for adult degenerative scoliosis including the Simmons classification system, the Aebi system, the Faldini working classification system, the Schwab system, and the Scoliosis Research Society (SRS) system. The presented classification systems may be correlated to the stiffness parameters found in the proposed study.

2.3.1. Simmons Classification System

The Simmons classification system classifies two types of degenerative scoliosis. The first type (Type I) includes no or minimal rotational deformity and the second type (Type II) includes a superposition of degenerative scoliosis on a preexisting scoliosis with noticeable rotational deformity and loss of lordosis (Simmons 2001).

2.3.2. The Aebi System

Currently, adult scoliosis can be diagnosed within the Aebi system as 3 different types: Primary degenerative scoliosis (Type 1), progressive idiopathic scoliosis (type 2), and secondary degenerative scoliosis (type 3) (Aebi 2005). The main advantage of this classification system is its ability to predict the natural cause of the deformity. However, the detailed features of the deformity are not identified (Faldini, Di Martino et al. 2013).

2.3.2.1. Type 1: Primary Degenerative Scoliosis ("de novo")

Scoliosis due to asymmetric degenerative disc changes is generally classified as type I and can be accompanied by a frontal plane deviation and rotation of the facet joints. Generally, the apex of the curve is located in the lumbar spine, between L2 and L4. Sagittal misalignment, usually in the form of a flat back or lumbar kyphosis, is responsible for severe back pain in patients. One study showed that 48% of examined degenerative patients lost their lumbar curve (Grubb and Lipscomb 1992). The disc degeneration can eventually lead to spondylosis, disc bulging, osteophytes, ligamentum flavum calcification, and facet joint arthritis with hypertrophic capsules and calcification (Ruiz Santiago, Alcazar Romero et al. 1997, Aebi 2005).

2.3.2.2. Type 3: Secondary Degenerative Scoliosis

The adult secondary degenerative scoliosis is generally located in the thoracolumbar, lumbar, and lumbosacral portion of the spine and may be idiopathic, neuromuscular, or congenital or caused by a lumbosacral anomaly (Aebi 2005). Pelvic obliquity or leg length discrepancies can also cause the spine to deviate in the coronal plane without any significant rotation. Also, bone weakness due to osteoporosis can cause vertebral fractures which may lead to an asymmetric loading situation complimented scoliosis and/or kyphosis.

2.3.3. The Faldini Working Classification System

The Faldini system was created to properly plan adult degenerative scoliosis surgery by standardizing the categorization of patients and curve types. Curves can be defined by either stable curves (A-type curves) and unstable curves (B-type curves) (Faldini, Di Martino et al. 2013).

2.3.3.1. A-type: Stable Curves

The A-type curves result from asymmetric facet joint degeneration involving laminae, ligaments, and intervertebral discs. The mobility of the functional spinal unit is reduced and kept in a fixed lateral deformity. The A-type curves can be grouped into 4 categories: A1, A2, A3, A4. A1 curves include facet hypertrophy with foraminal stenosis, A2 curves include facet hypertrophy with central stenosis, A3 curves include intervertebral disc degeneration, and A4 curves are a mix of the other three curves.

2.3.3.2. B-type: Unstable Curves

The B-type curves result from a developmental degeneration of facet joints, laminae, flavum ligaments, and intervertebral discs increasing to a larger functional spinal unit physiological range of motion. Like the A-type curves, the B curves can also be subgrouped. B1 curves exhibit hypermobility due to facet joint degeneration. B2 curve instability is caused by intervertebral disc degeneration. B3 curves include a mix of B2 and B1 Curves. B4 unstable curves are results of more complex cases of sagittal plane imbalance.

2.3.4. The Schwab System

The Schwab system classified a clinical series of 947 adult scoliosis patients based on correlating radiographic parameters (frontal plane Cobb angle, apical level of deformity, sagittal plane lumbar alignment, and intervertebral subluxation) with outcome measures such as the Oswestry Disability Index and the Scoliosis Research Society outcome measure (Schwab, Farcy

et al. 2006). The apical level of the deformity was separated into five groups: type I (thoracic only), type II (upper thoracic major curve with apex at T4-T8), type III (lower thoracic major curve with apex at T9-T10), type IV (thoracolumbar major curve with apex at T11-L1), and type V (lumbar major curve with apex at L2-L4). However, this study will only encompass type V scoliotic patients. Modifiers were instituted based on the magnitude of lumbar lordosis and intervertebral subluxation at any level. These modifiers may be correlated to the data collected from the study. The Schwab classification system had shown a significant correlation with patient management (Faldini, Di Martino et al. 2013).

2.3.5. The Scoliosis Research Society (SRS) System

The SRS system includes the classification of both the "de novo" and adult idiopathic scoliosis with superimposed degeneration with analysis of global balance, regional deformity, and focal degenerative changes within the deformity (Lowe, Berven et al. 2006). This classification also incorporates primary sagittal deformity, Scheuermann's kyphosis, trauma, loss of muscle tone, and osteoporosis. The coronal plane major curve types are separated into a single thoracic, a double thoracic, a double major, a triple major, a thoracolumbar, or a lumbar. Primary thoracic curves should be greater than 40^{o} while thoracolumbar and lumbar curves should be greater than 30^{o}.

The first regional modifier considers sagittal deformities such as regional kyphosis or hypolordosis. Lumbar degeneration modifiers were implemented to identify degenerative radiographic findings including evidence of disc narrowing, facet arthropathy, and degenerative spondylolisthesis or rotary subluxation greater than 3 mm in any plane. Imbalance in either the coronal or sagittal plane contributed to the third modifier to account for any global misalignment. The SRS classification system did not include clinical considerations such as pain symptoms, age, and comorbidities.

2.4. Stiffness Testing

A number of studies have examined the *in vivo* passive stiffness of the human torso. McGill et al. looked at the passive bending properties of the intact human torso in the three anatomical planes with flexion/extension, lateral bending, and axial rotation motions (McGill, Seguin et al. 1994). The authors were able to quantify the lumbar spine stiffness characteristics by applying a known torque and measuring the torso angular displacement. Another study, which employed similar experimental methods, defined the asymmetrical lumbar region passive tissue characteristics between people with and without low back pain (Gombatto, Norton et al. 2008). Instead of quantifying only stiffness values, the authors used passive elastic energy to describe the differences between people with and without back pain. Subjects with back pain demonstrated a greater asymmetry of passive elastic energy than people without lower back pain. A study demonstrating the effects of prolonged sitting on the passive flexion stiffness in the *in vivo* lumbar spine found that stiffness increased in men only after 1 hour of sitting while stiffness varied in women over a 2 hour trial (Beach, Parkinson et al. 2005). The "low stiffness" and "high stiffness" zones were only compared in this study, which are the regions on the moment-angular displacement plot where the spines exhibit low and high stiffness characteristics.

2.4.1. The Neutral Zone

Panjabi (1992) defined the spinal load displacement curve using terms including the neutral position, range of motion (ROM), neutral zone (NZ), and the elastic zone (EZ). The neutral position is considered the spinal posture in which the internal stresses and postural muscular effort are minimized and ROM defines the entire physiological intervertebral motion referenced from the neutral position. The ROM region where there is minimal internal resistance is considered the NZ and where there is significant internal resistance is considered the EZ. The

author measured the neutral zone of the spinal specimen with three static loading times to estimate maximum physiological load. Load displacement values are recorded only during the 3rd load cycle to account of viscoelastic creep. The residual displacements right before the third load cycle is considered the end of the neutral zone. This also can be applied in the opposite direction to define the total neutral zone. However, the load applied and loading time history is arbitrary. Considering an *in vivo* study that employs unique subjects, the NZ should not be dependent on an arbitrary maximum load.

Wilke, Wenger et al. (1998) examined the NZ with a dynamic loading situation in which an *in vitro* specimen was brought to one end range of motion first and then the opposite end range of motion through a dynamic movement. Again, there were three loading cycles to reduce the viscoelastic properties. The authors define the NZ as the difference in angulation at zero load between the opposite motion phases as displayed in Figure 2.7. The authors also noticed the loading rates can have considerable effects: slower rates may induce creep effects while faster rates may increase the inertial contribution to the system. There is no arbitrary loading in this study, but the deformation at zero load may not identify the borders of the neutral zone because, for example, the spinal motion segments may not have been properly located in its neutral position causing the neutral zone to shift (Smit, van Tunen et al. 2011). This characteristic would be evident in an *in vivo* scoliotic spine since the spine is already in a deformed position. Also the NZ is considered the region at which the spine offers the least resistance, which may be defined where the stiffness of the spine is minimized. The stiffness of the spine at a load greater than the zero load limit (see Figure 2.7) may be relatively the same, meaning that the spine does not offer an increase of resistance. Instead, the point at which the spine increases it stiffness substantially should be considered the limit of the NZ.

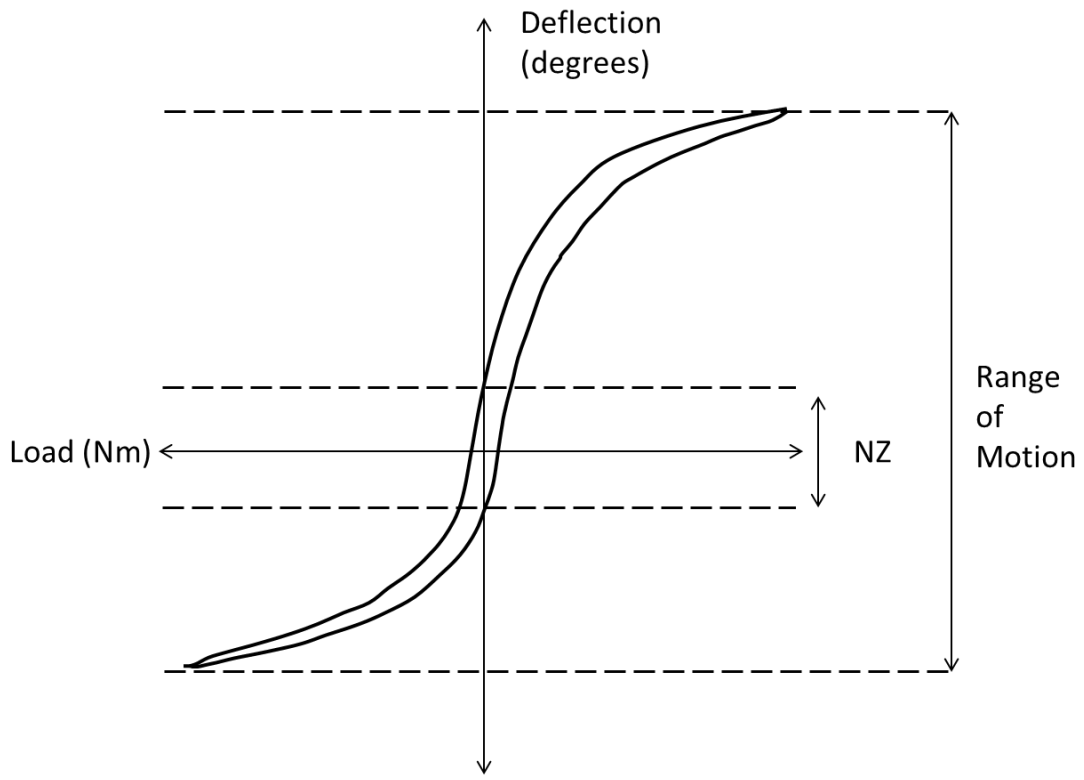

Figure 2.7 Wilke, Wenger et al. (1998) representation of the neutral zone and the range of motion. The bounds of the neutral zone are defined at the points of zero load.

Another study defined flexibility as the slope of the tangent line along a linear portion of the torque deflection curve that had the highest coefficient of determination (6 sequential data points) (Spenciner, Greene et al. 2006). The NZ was then defined as the intersection of the flexibility tangent line with the zero loading axis (y axis), shown in Figure 2.8. This method depends on the defined end ROM based on the desired load applied. With a larger ROM, the slope of the flexibility line will be smaller resulting in the larger neutral zone. The converse is true for a smaller ROM. Thompson, Barker et al. (2003) used a fourth order polynomial to define the load deflection data. The gradient of this fourth order system quantified the stiffness and the NZ limited were defined when the gradient breached ± 0.05 N-m/^{o}. However, these limits were arbitrarily chosen as well.

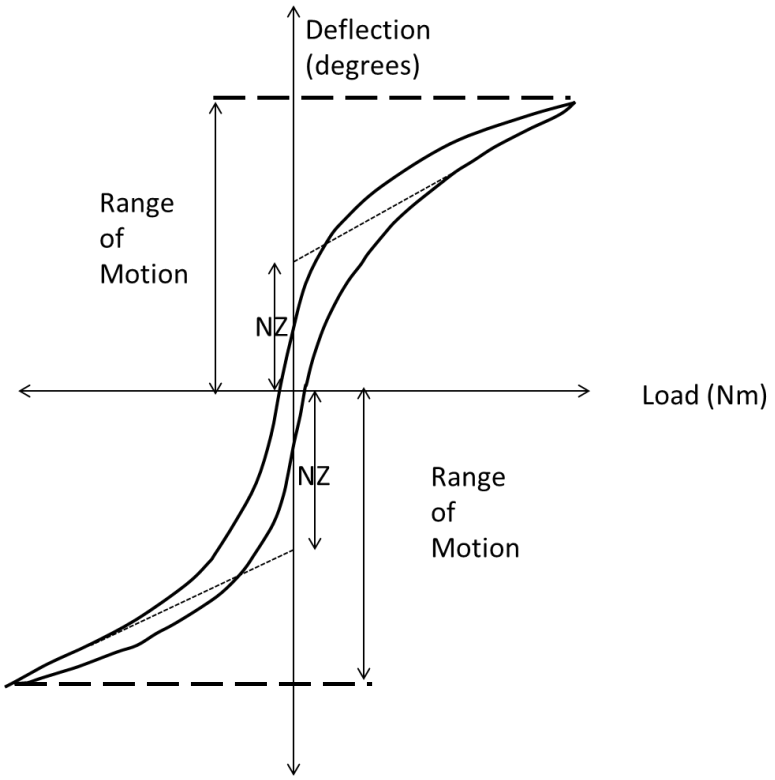

Figure 2.8 Spenciner, Greene et al. (2006) visual representation of the neutral zone.

Smit, van Tunen et al. (2011) proposed a new definition of the neutral zone that was independent from of an arbitrarily chosen maximum load and starting point of the load deflection curve and accounted for the asymmetry for the load deflection curve. To overcome noise in the raw load-deflection data, the authors fit the data to a double sigmoid function to filter the noise and to analytically represent the non-linear characteristics of the data. A straight line was fit over the load-displacement curve to define the neutral zone stiffness. With this method, the independent neutral zones can be determined on both sides of the load-deflection curves, such as flexion vs. extension, right lateral bending vs. left lateral bending, and right axial torsion vs. left axial torsion. Another study employed the Smit et al. NZ analysis and was able to define their NZ range well (Howarth, Gallagher et al. 2013).

3. METHODS

This chapter details the experimental setup that addressed the objectives of the study to the hypotheses. The participants, apparatus, instrumentation, experimental procedure, and data analysis are provided in the subsequent sections.

3.1. Human Samples

The subject population focused on adult ages 18-75 including lumbar degenerative scoliotic subjects and control subjects. Scoliotic subjects included individuals with Cobb angles between 15-75^{o} defined the frontal plane. Both female and male subjects were accepted. Although scoliosis is more prominent in females, the progression of scoliosis does not correlate with gender (Grubb and Lipscomb 1992, Seo, Ha et al. 2011). Both left and right deformations across the sagittal plane were also accepted. Scoliotic and healthy subjects required a BMI < 30 to participate and could not have extreme lower back pain (VAS >7). Scoliotic and control subjects were excluded if they suffered from a systemic inflammatory condition, ankylosing spondylitis, pulmonary conditions, and/or congestive heart failure. Subjects with spondylolisthesis, history of spinal fracture, or history of spinal surgery were also excluded from the study as changes in vertebral stability due to these conditions may alter the spine stiffness and confound the results. Participants completed an informed consent procedure approved by the Carilion Clinic Institutional Review Board. Because the scoliotic subjects were referred from a scoliosis specialist, radiographic data necessary to describe the type of scoliosis was already provided. The experimental sessions commenced both at the Carilion Clinic, in Roanoke, Va and in the Occupational Biomechanics and Ergonomics Laboratory at Virginia Tech.

Sample sizes were estimated with a power analysis adopted from results of a study that compared the lumbar stiffness of patients with and without lower back pain (Brodeur and DelRe

1999). The meaningful effect from this study was the significant increase or decrease of lumbar stiffness between symptomatic and asymptomatic subjects. The results of the power analysis assuming a significance of $\alpha = 0.05$ (2 tail test) are shown in Figure 3.1. At a power of 0.8, the estimated sample size was 70 total patients, 35 asymptomatic patients and 35 symptomatic patients. However, the power study did not compare manipulated spine mechanics, which may affect the stiffness more than just pain symptoms. A lower power value was hence considered as the current study focused on the altered mechanics of the spine which may affect the mechanics of the lumbar spine more than symptomatic pain reporting alone. At a 0.7 power level, a total sample size of 56 was required. At a 0.6 power level, a total sample size of 46 was required. To satisfy these a priori assumptions, 23 subjects from the healthy and scoliotic population were desired. However, the difficulties in recruiting subjects resulted in 14 scoliotic subjects and 17 control subjects tested. Table 3.1 displays the demographics of the subjects recruited. Mean and standard deviation data for both subject groups are displayed in Table 3.2.

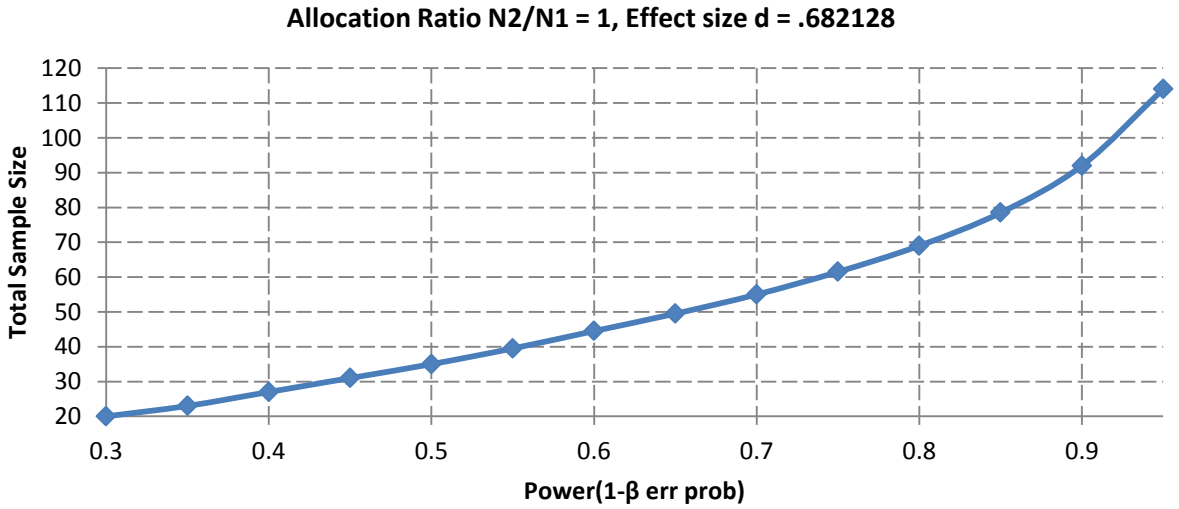

Figure 3.1 Power study adapted from (Brodeur and DelRe 1999)

Table 3.1. Subject demographics. Subjects without scoliosis values (Apex Direction, Cobb Angle, and Apex Level) were the recruited controls

Subject	*Gender*	*Age*	*Height (inches)*	*Weight (lb)*	*Apex Direction*	*Cobb Angle*	*Apex Level*
1	F	51	66	171	-	-	-
2	M	27	70	135	-	-	-
3	F	24	65	170	-	-	-
4	F	37	61	143	-	-	-
5	M	29	73	205	-	-	-
6	M	23	72	160	-	-	-
7	F	25	66	145	-	-	-
8	M	32	70	165	-	-	-
9	M	54	73.5	196	-	-	-
10	F	25	68	163	-	-	-
11	M	24	70	150	-	-	-
12	F	26	62	120	-	-	-
13	M	22	74	165	-	-	-
14	F	31	67	160	-	-	-
15	M	23	70	186	-	-	-
16	F	30	68	153	-	-	-
17	M	27	73	185	-	-	-
18	F	50	61	128	Left	73	L1-2
19	F	48	57	195	Left	35	L2-3
20	F	71	63	121	Right	82	L2
21	F	50	65	178	Right	45	L1-2
22	F	65	60	139	Left	19	L3-4
23	M	63	64	132	Left	48	L2
24	F	50	68	166	Left	21	L1-2
25	M	60	59	129	Left	41	L2-3
26	F	76	66	160	Right	33	L3-4
27	F	71	60.5	135	Right	30	L5
28	F	66	63.5	137	Right	31	L2-3
29	F	78	65	131	Right	67	L2
30	M	63	58	178	Left	28	L2
31	F	52	63	104	Left	45	L2

Table 3.2 Mean and standard deviation data compared between tested groups

	Mean(Std)		
	Age (years)	Height (in)	Weight(lb)
Control	30.00(9.32)	68.74(3.89)	163.06(21.84)
Case	61.64(10.27)	62.36(3.21)	145.21(25.88)

3.2. Apparatus and Instrumentation

3.2.1. Apparatus

The experimental setup was adapted from previous *in vivo* trunk passive stiffness studies (McGill, Seguin et al. 1994, Scannell and McGill 2003, Beach, Parkinson et al. 2005, Gombatto, Norton et al. 2008). As such, the subjects participated in three tests that quantified the kinematics of the lumbar spine across each anatomical plane of motion. The first test required subjects to lie in a supine position where the lower extremities were fixed in position and the legs were restrained. The upper torso (the head to the bottom of the rib cage) was fixed in a moveable cradle. The under surface of the cradle was composed of Plexiglas® and was supported by a distribution of ½" nylon bearings. The bearings allowed for the cradle to "float" by assuming minimal frictional resistance. In this setup, the subject was moved with a lateral bending moment, where a majority of the movement would occur in the lumbar spine. The apparatus setup is shown in Figure 3.2.

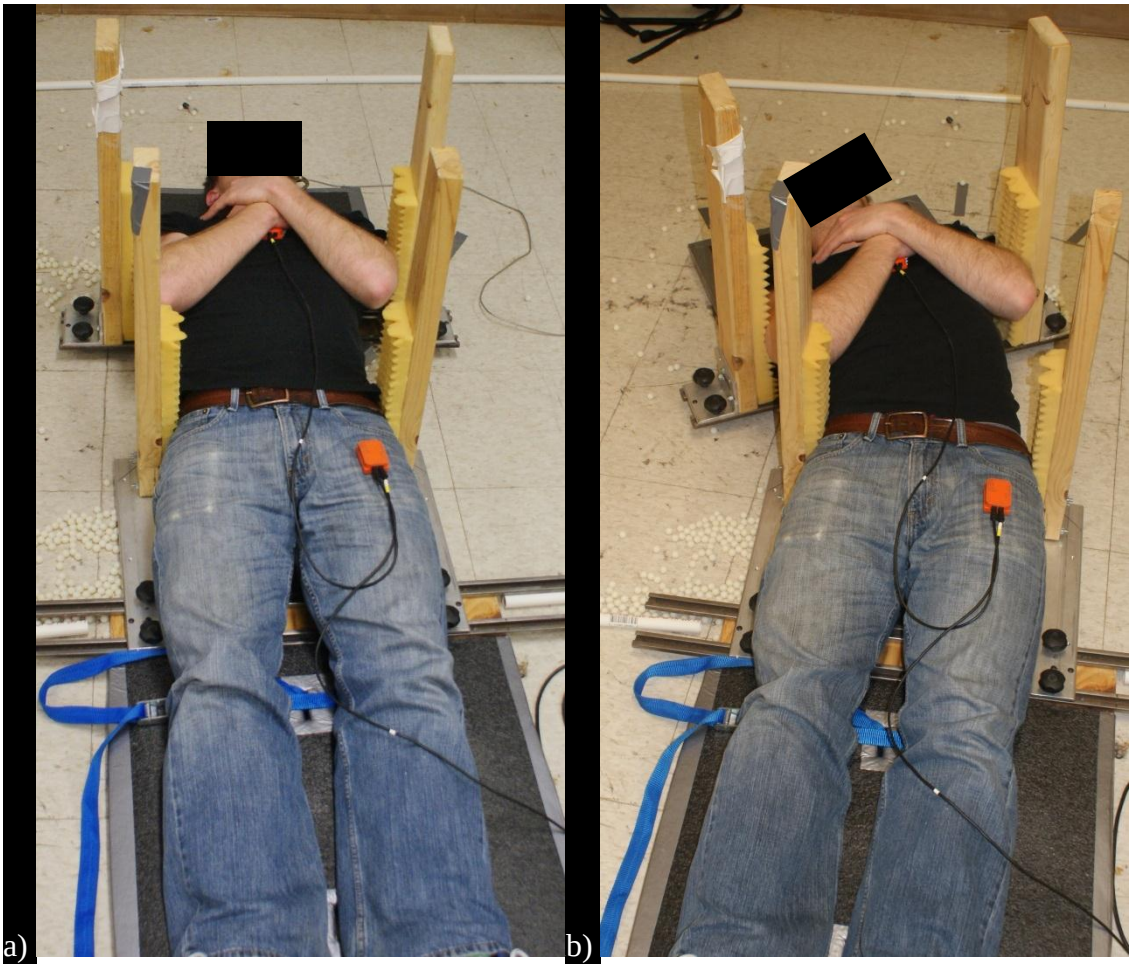

Figure 3.2 a) Subject fixed in the neutral position on the cradle. b) Torque induced on the cradle creates angular displacement.

The second test used the same setup except the subject was positioned on his or her side and a flexion/extension moment was then applied. Again, the majority of the flexion and extensions movements occurred in the lumbar spine. Flexion and extension positions are pictured in Figure 3.3 and Figure 3.4, respectively. Any further lateral curvature of the spine was avoided my placing cushions underneath the subjects' waists, knees, and head.

Figure 3.3 Subject fixed in a flexed torso position

Figure 3.4 Subject fixed in an extended torso position

The final test included an axial rotation movement where the rib cage was fixed on two underarm supports as the subject knelt on an ergonomic chair (Flash Furniture ®), which was mounted on a rotating platform. The pelvis, hips, and shanks rotated as a single unit while the upper torso remained stationary, only allowing lumbar spine twist. Torque was induced by a

force directed tangential to the rotating platform. The torso was fixed to a stationary support, shown in Figure 3.5.

Figure 3.5 Subject fixed to a stationary support with the use of a strap. Another strap (not shown here) covers the hips and wraps around the chair to fasten the lower extremities to the rotating platform. The bar attached vertically to the load cell in this photograph was longer than the actual testing length. This figure is meant to clearly illustrate the testing apparatus.

The coupled motion of the scoliotic spine indicates that one directional loading (i.e. lateral bending) may induce viscoelastic creep effects on a different anatomical motion (i.e. axial rotation). As such, the resultant measured directional stiffnesses may be dependent on the order of the testing protocol. To remove this effect, the order of the testing procedures was counterbalanced across participants.

3.2.2. Instrumentation

To ensure the tests only included passive spine characteristics, a biofeedback system indicated when subjects were voluntary activating their spinal musculature. Bipolar surface electrodes with inter-electrode separation of 2 cm were placed on the external oblique (Lateral most portion of the muscle oriented parallel of muscle fibers) and lumbar erector muscles (L3 Level) to measure the electromyography (EMG) activity of the muscles.

Angular displacements were obtained with two Motion Trackers (MTx)®, or inertial motion sensors (IMS), manufactured by XSens Technologies. One IMS was fastened to the pelvis and one inertial motion sensor was fastened to the torso. Each IMS was capable of tracking 3-D kinematic data (orientation and position) in a world coordinate-based frame. The Xbus Master® supplies power to the MTX's and samples digital data from the sensors. The Xbus Master then transfers/stores data from the sensors to a PC. The force applied on the cradle and rotating platform was measured with a unidirectional load cell (SP-500, Interface, Scottsdale, AZ). In the lateral bend and flexion/extension trials, the load cell was fixed to the cradle via a ball and socket joint and an IMS sensor was attached to the load cell to track the angle of force application to relative to the cradle. A schematic of the lateral bend setup is shown in Figure 3.6. In the axial twist trial, the load cell measured a force directed tangential to the rotation. Force, EMG (RMS converted in hardware) and kinematic data were software synched and collected at 100 Hz and were low-pass Butterworth filtered at 5 Hz, which was determined through residual analyses. Force data was measured in Newtons (N) and angular data was measured in degrees (^{o}).

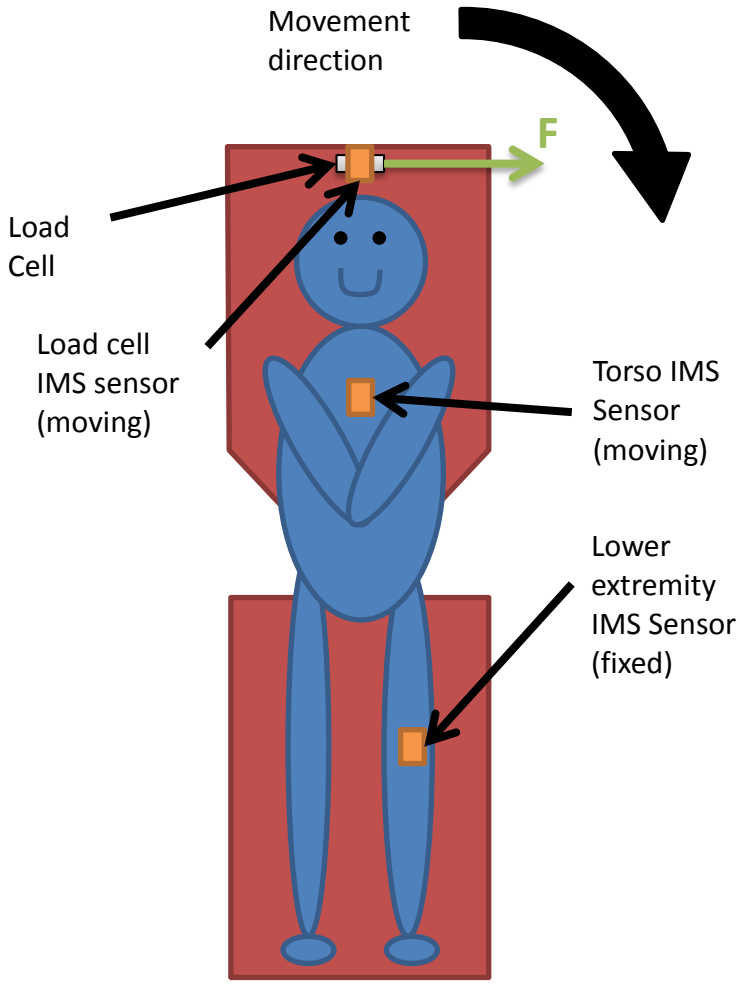

Figure 3.6 In the lateral bend setup, the lower extremities were fixed. The relative angle of torso deflection was measured with the torso IMS and the lower extremity IMS. The load cell measured the force acted on it and the load cell IMS detected what direction the force was being applied relative to the body.

3.2.3. Experimental Procedure

Three continual trials were performed for each of the three directional movements, flexion/extension, right/left lateral bending, and clockwise(CW)/counterclockwise(CCW) rotation. In the lateral bend setup, the research assistant first aligned the left and right anterior superior iliac spine (ASIS) with the superior face of the wooden post. The ASIS is a landmark anterior to the L5-S1 vertebral joint approximately in the same transverse plane. The wooden posts on the stationary apparatus were then adjusted to rigidly fix the pelvis while maintaining

subject comfort. Straps were then fastened around the thigh and shank to minimize lower extremity movement. The moveable cradle was then adjusted such that the bottom of the moveable cradle was posterior to the bottom of the rib cage. After positioning the subject on the cradle, the wooden posts on the cradle were then slid medially to fix the upper torso the cradle. Subjects were then instructed to cross their arms over their chest. The flexion/extension trials commenced on the same apparatus as the lateral bend trials. The same anatomical landmarks in the lateral bend test were used to position subjects. However, subjects were required to lay on their side for the flexion/extension trial.

In the axial twist setup, subjects were placed in the ergonomic chair and the research assistant fastened the lower extremities to the chair with a belt. The underarm rests, which are shown in Figure 3.5, were then moved medially or laterally to accommodate for the width of each subject. Each subject was then instructed to rest their upper torso on the underarm supports. The underarm supports were then adjusted vertically to ensure a vertically erect spine. A strap attached to the underarm support apparatus was then wrapped posteriorly around the subject to minimize relatively movement between the upper and lower extremities.

After positioning subjects in the apparatus, the research assistant recorded baseline EMG levels as subjects were instructed to relax as much as possible. This was performed for each trial to account for any involuntary spinal muscular activation. During each of the tests, trunk muscles were considered relaxed when the EMG levels remained below 2 standard deviations of the baseline EMG level. An auditory tone would sound from the data acquisition computer if the subject was considered active. If EMG levels surpassed the threshold for more than 10% of the trial, the trial was discarded and repeated as necessary.

Once baseline EMG was recorded, the research assistant practiced the particular movement with the subjects to understand the limits of muscle relaxation and the range where no more torque should be applied based on subject comfort. The angular displacement at which the level of discomfort was 5 or greater on a VAS scale determined as the limits of range of motion for each participant. If the subject did not reach a discomfort level of 5 or greater, 30^{o} was used as an upper bound from the resting position. Therefore, the maximum total range of motion was 60^{o}. In the lateral bend and flexion/extension trials, the research assistant applied a force to the cradle superior to the head to induce a torque on the lumbar spine. In the axial twist, the research assistant applied a force tangent to the center of rotating platform to induce a torque at the lumbar spine.

In all of the trials, the speed of the movement was kept at a constant 5^{o}/s among all of the participants through the use of a metronome and a large "protractor". This speed was chosen based on the preliminary analysis that can be found in the Appendix, Section 1.A.1. The data collection began when the subject was in a rested position. Depending on the test, the research assistant brought the subject to one end range of motion and then to the other range of motion. This process continued for a maximum of ten cycles. A single trial was performed for each of the anatomical movements.

Because of the viscoelastic properties of the spine, the displacement/moment relation may be affected by creep (McGill and Brown 1992, Little and Khalsa 2005). The *in vivo* lumbar spine represents a 1^{st} order system of creep during a static 20 minute flexion and then release (McGill and Brown 1992). However, it was assumed that the cyclic loading used in this study would cause a lower creep rate as compared to a static flexion condition (Little and Khalsa 2005). Furthermore, Fung (1984) explained that soft tissues in the constant loading response can be

preconditioned to remove the viscoelastic creep properties. Other studies have employed this principle and preconditioned the spine to remove the creep in the beginning of the trial, creating more consistent data (Wilke, Wenger et al. 1998, Thompson, Barker et al. 2003, Spenciner, Greene et al. 2006, Bisschop, Kingma et al. 2013). As such, the first two cycles were considered preconditioning movements. Only data after the first two cycles were analyzed for this study.

3.3. Data Analysis

3.3.1. Torque and Displacement Calculations

In this investigation, a lumped parameter linear system was applied to the human torso as described in Equation 1.

$$M = I\ddot{\theta} + b\dot{\theta} + \mathrm{k}\theta \qquad [1]$$

M is the sum of the moments about the pelvis, I is the inertial properties of the entire torso, b is the damping characteristics of the lumbar spine, k is the stiffness characteristics of the lumbar spine, and θ is the angular deflection of the torso. To calculate the stiffness of the lumbar spine from Equation 1, the inertial properties of the system were minimized. The inertial coefficient was considered insignificant due to the constant angular velocity and was eliminated from analysis. Because the angular velocity was constant among all subjects, a damping coefficient could not be computed. Therefore, the damping coefficient was also ignored in this study. The relationship between the applied moment and the resultant deflection was estimated with a non-constant stiffness value of k. The moment arm in the lateral bend and flexion/extension was measured from the point of application of the force to the L5-S1 joint. This moment arm was assumed constant throughout the movement for a given subject. Because of the assumed zero friction the lateral bend and flexion/extension, any friction force was not accounted for in the

data analysis. The axial twist moment arm was measured at a constant of 0.2974 meters. In addition, the axial twist apparatus incurred a constant friction force of 3 N on the load cell and was compensated for during analysis.

The IMS can be set to output the angular data in eularian angles, quanterions, or rotational matrices. However, to encompass the 3-D kinematic data, rotational matrices recorded by the hip and torso sensors were compared to calculate the absolute relative angular displacements between the fixed hip and moving torso. A rotation matrix can be expressed by Equation 2.

$$\begin{bmatrix} cos\theta cos\phi & sin\psi sin\theta cos\phi - cos\psi sin\phi & cos\psi sin\theta cos\phi + sin\psi sin\phi \\ cos\theta sin\phi & sin\psi sin\theta sin + cos\psi sin\phi & cos\psi sin\theta cos\phi - sin\psi cos\phi \\ -sin\theta & sin\psi cos\theta & cos\psi cos\theta \end{bmatrix} \quad [2]$$

Theta (θ), phi (ϕ), and psi (ψ) represent the sensor roll, pitch and yaw angles, respectively. This study only examined the yaw angle of the sensor as it represented the desired angular displacement between the two IMU sensors. Roll and pitch angular displacements in the present were assumed insignificant as compared to the yaw displacement.

The relative rotation matrix between both of the sensors can be computed from the dot product of the two matrices, shown in Equation 3.

$$\boldsymbol{R_r} = \boldsymbol{R_{hip}}\boldsymbol{R_{torso}}^T \quad [3]$$

$\mathbf{R}_r$ is the rotation matrix between the two sensors, $\mathbf{R}_{torso}$ is the rotation matrix of the torso IMS sensor in the global coordinate system, and $\mathbf{R}_{hip}$ is the rotation matrix of the hip IMS sensor in the global coordinate system. Similarly, the relative angle between the rotational torso sensor and the load cell sensor (lateral bend and flexion/extension trials only) can be calculated through the same method, shown in Equation 4.

$$\boldsymbol{R_d} = \boldsymbol{R_{torso}}\boldsymbol{R_{LC}}^T \quad [4]$$

$\mathbf{R}_d$ is the rotation matrix expressing the difference in angles, $\mathbf{R}_{torso}$ is the rotation matrix of the torso IMS sensor in the global coordinate system, and $\mathbf{R}_{LC}$ is the rotation matrix of the load cell IMS sensor in the global coordinate system. ϕ_d is the relative angle between the load cell angle and the torso angle, as seen in Figure 3.7. The torque (N-m) produced in the lateral bend and flexion/extension trials was calculated with Equation 5. The torque (N-m) produced in the axial twist trials was calculated with Equation 6.

$$\tau = 0.2974 * F \quad [6]$$

$$\tau = (Moment\ Arm) * F * cos\phi_{LC} \quad [5]$$

$$\tau = 0.2974 * F \quad [6]$$

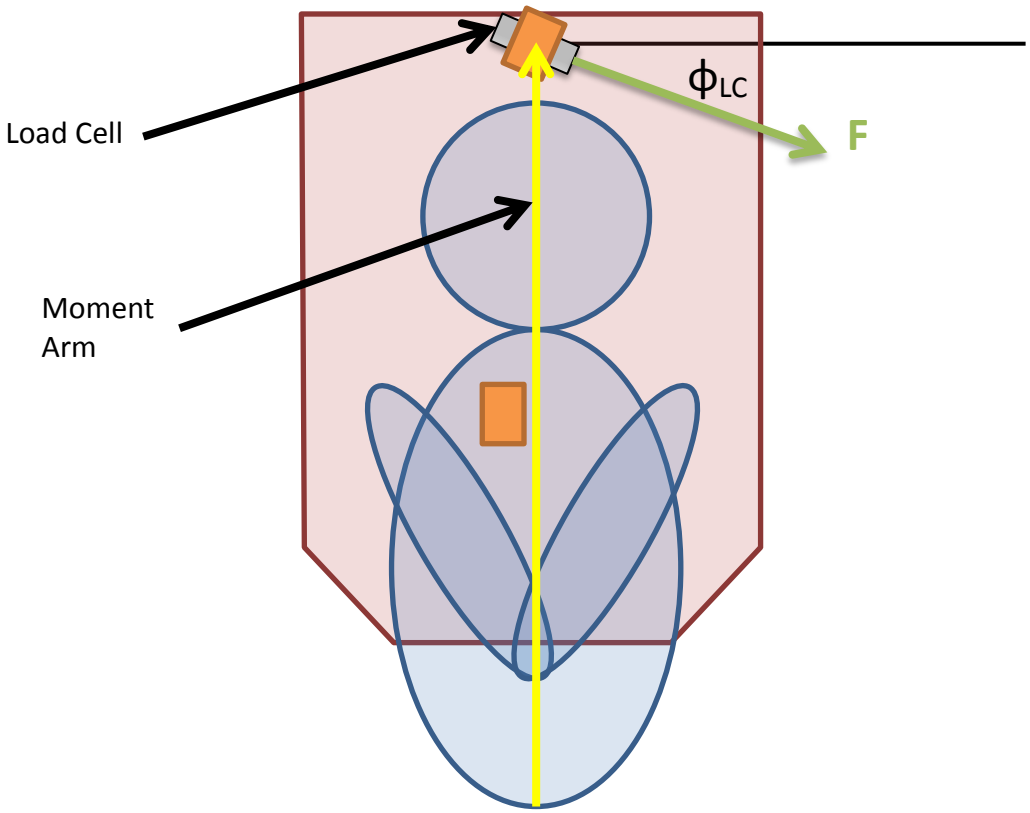

Figure 3.7 The lateral bend and flexion/extension trials calculated the torque using a moment arm measured from L5-S1 joint to the load cell.

It should be noted that the magnetic field in the laboratory may have caused the measured angles to "drift" since they are based on a magnetic north. The velocity of the "drift" was approximately constant. A linear regression was fit to the peaks of the kinematic data and was used to correct for the data drift. However, this corrective method assumed the research assistant reached the same peak angle during each pass.

3.3.2. Non-Linear Stiffness Model

The non-linear stiffness characteristics of the lumbar spine were computed from the corresponding torques and angular displacements. A curve fitting technique from Smit, van Tunen et al. (2011) was then used to determine the stiffness and neutral zone of the spine. Because of the viscoelastic properties of the spine, the load deflection curve should resemble a

hysteresis loop as shown in Figure 3.8. The bottom and top curves can each individually be fit to a double sigmoid function shown in Equation 7, where τ is the induced torque.

$$\theta = \frac{1}{1 + e^{-(a_1 + b_1 * \tau)}} * c_1 + \frac{1}{1 + e^{-(a_1 + b_2 * \tau)}} * c_2 + d \qquad [7]$$

The parameter b influences the slope of Equation 7 and the parameter c determines the ROM of the torso. Parameters a and d shift the curve horizontally along the loading axis or vertically along the displacement axis.

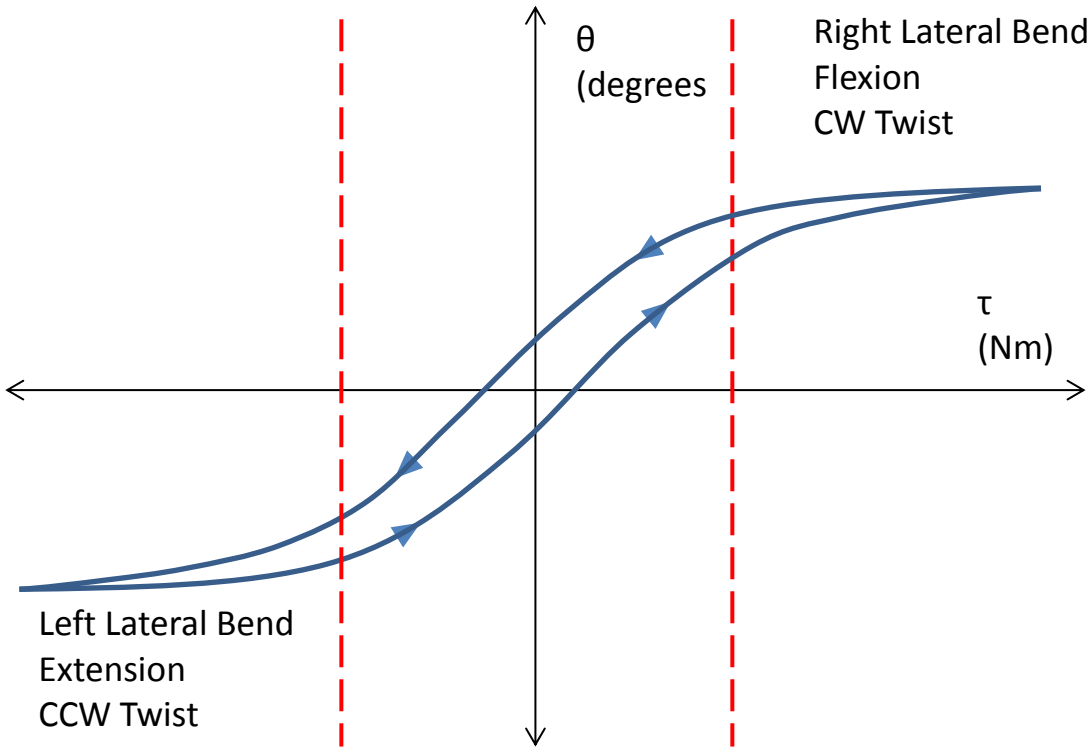

Figure 3.8 A theoretical hysteresis loop. The arrows represent the loading directional loading during each trial. The dashed lines represent where the 2nd derivative of the curves reach a local extrema.

The data from each trial was imported into MATLAB and separated into six total loading directions—left lateral bend to right lateral bend (LtoR), right lateral bend to left lateral bend (RtoL), flexion to extension (FtoE), extension to flexion (EtoF), clockwise twist to

counterclockwise twist (CWtoCCW), and counterclockwise twist to counterclockwise twist (CCWtoCW) to fit separate curves. The curve fitting tool (cftool) from MATLAB was used to fit each of the curves. The fitting program used a nonlinear least square method with a bisquare weights and a Levenberg-Marquardt algorithm. The coefficients' starting points were randomized in a range from 0 to 1 and the solved coefficients were unbounded. Because each curve fit routine solves for 7 coefficients, the curve fitting tool calculated various solutions based on the starting points of the coefficients. As such, the solution with the greatest coefficient of determination (R^2) value was considered to be the best fit of the data.

The derivative of Equation 7 describes the inverse of the spinal stiffness, or compliance. The position along the curve where the rate of change of stiffness is minimized determines the limits of the neutral zone since that is the location where a significant change in stiffness becomes the most apparent. These limits can be found by the inflection points of the second derivative of Equation 7, which is illustrated in Figure 3.9.

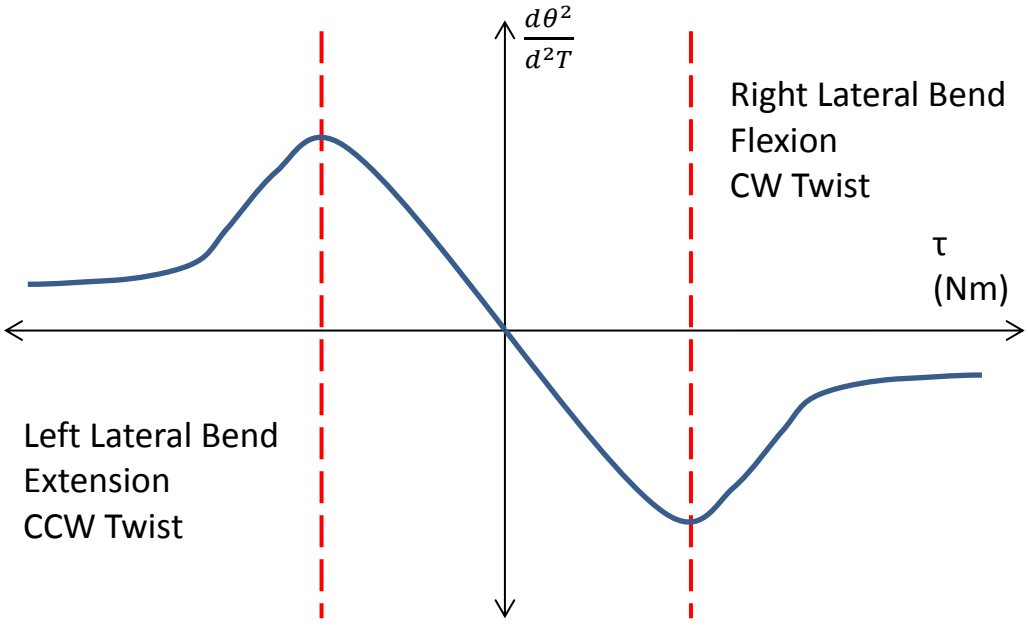

Figure 3.9 The second derivative of one of the curves from Figure 3.8. The area between the two dashed lines is considered the neutral zone.

The stiffness of the spine was quantified both inside and outside the neutral zone. The stiffness inside the neutral zone was considered constant while the stiffness outside the neutral zone will exhibit non-linear behavior. The neutral zone data was fit with a linear regression and the slope of the line was considered the inverse of the stiffness coefficient. This is similar to the methods of Smit, van Tunen et al. (2011), who also fit the neutral zone with a linear regression, producing very good results. To quantify the stiffness outside of the neutral zone, Equation 8 from McGill, Seguin et al. (1994) was manipulated to yield Equation 9. The inverse of the derivative of Equation 9 represents the stiffness outside of the neutral zone.

$$\tau = \alpha * e^{\beta\theta} \quad [8]$$

$$\theta = \frac{1}{\beta} * \ln(\frac{\tau}{\alpha}) \quad [9]$$

$$k = (\frac{d\theta}{d\tau})^{-1} = \tau * \beta \quad [10]$$

According to Equation 10 the stiffness of spine will increase as the torque induced on the spine increases. However, the rate at which the stiffness will increase is based on the magnitude of parameter β. Therefore, the β parameter was used in comparing the stiffness between populations and anatomical loading directions.

Because of the presence of hysteresis, the unloading and loading fits of Equation 9 were different. Equation 9 was fitted to the loading and unloading curves on each side of the neutral zone. Each curve should theoretically result in different α and β parameters. This concept is illustrated in Figure 3.10. Because the width of the neutral zone will have an effect on the starting portion of the non-linear data points, each of the curves were zeroed before a fit was computed.

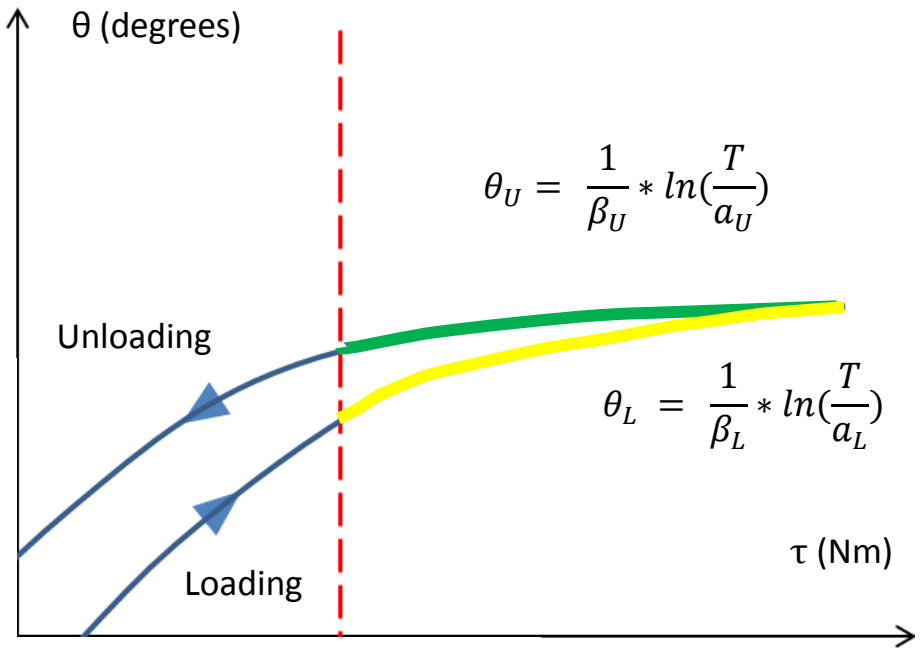

Figure 3.10 Both the loading and unloading fits can be found outside of the neutral zone. L subscript represents loading variables and R subscript represents unloading variables.

3.4. Statistical Analysis

Paired-sample t-tests were performed on NZ widths, NZ stiffnesses, α parameters, and β parameters between corresponding loading/unloading conditions for each anatomical motion (i.e. Right Lateral Bend β_L vs Right Lateral Bend β_U). This would determine if the parameters between unloading and loading were different due to the theoretical hysteresis loop. If there was no significant difference between the two dependent variables, the two variables corresponding to each subject would then be averaged to represent the mechanical parameters for later analyses (i.e. [Right Lateral Bend β_L + Right Lateral Bend β_U]/2 = Right Lateral Bend β). If a significant difference existed, the loading cycle parameters would be used in the later analyses (i.e. Right Lateral Bend β = Right Lateral Bend β_L).

Originally, the stiffness within the neutral zone, width of the neutral zone, overall outside NZ stiffness, and stiffness asymmetries of the healthy and scoliotic patients were compared

independently, using two way, mixed factor analysis of variance (ANOVA – between factor of group, within factor of direction) to determine if the presence of scoliosis affects the stiffness characteristics in the lateral bend, flexion/extension, and axial rotation directions. However, with missing subject data, either with uneven subject population or unacceptable fits, the ANOVA could not be calculated. A generalized estimating equation (GEE) method was used to accommodate for the missing parts of data. To use this model, the data was assumed to be missing completely at random. A GEE model to compare stiffness within the neutral zone, width of the neutral zone, overall outside NZ stiffness, and stiffness asymmetries between control and scoliotic populations was performed for each anatomical movement. Overall outside NZ stiffness was computed from the average of the β parameter within each anatomical direction (ie. average of lateral right side β and lateral left side β). Stiffness asymmetries were expressed with the asymmetry stiffness index (ASI). The index, defined in Equation 11 expresses the ratio of the β parameter between opposite loading sides for each subject.

$$\mathrm{ASI} = \frac{\beta_G}{\beta_L} \qquad [11]$$

The β_G parameter represents the greater value between the two loading sides and β_L is the lesser value of the two sides. An increase in ASI represents an increase in the asymmetry between the β stiffness parameter. Correlation statistics were also performed between NZ width and NZ stiffness in each anatomical direction. An a priori significance value of α=0.05 was used for all analyses.

4. RESULTS

4.1. Goodness of Fit

The double sigmoid function provided a good fit to the experimental data in each of the three trials based on the R^2 values. An example of fitted data and residuals is shown in Figure 4.1. The second derivative corresponding to the curve in Figure 4.1 is illustrated in Figure 4.2 . Although this example curve fit the data well, each of the curves were inspected for any discontinuities or "oscillations" within the curve. The oscillations would appear as local extrema in the second derivative of the double sigmoid function and created more difficulty in determining the neutral zone of the data. Therefore, curves with the highest R^2 values and least amount of oscillations were chosen as the fits for the remainder of the analysis.

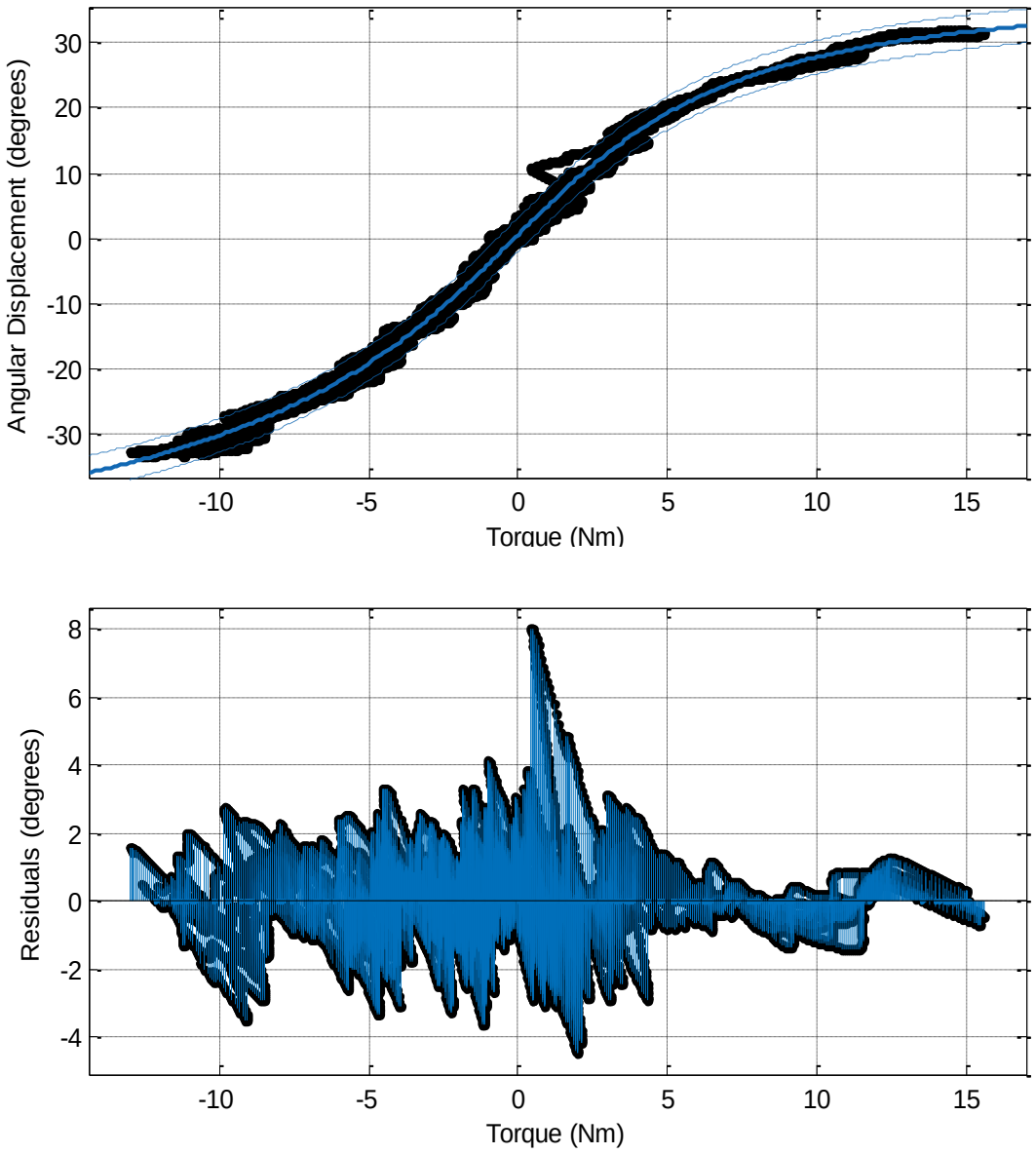

Figure 4.1 Subject 4 Left Lateral bend to Right Lateral bend. In the top plot, the black dots represent the experimental data of the entire trial. The blue solid line is the curve fit to the data and the dashed lines represent the bounds of 95% confidence interval of the fitted curve. The bottom plot shows the total residuals between the data and fitted curve.

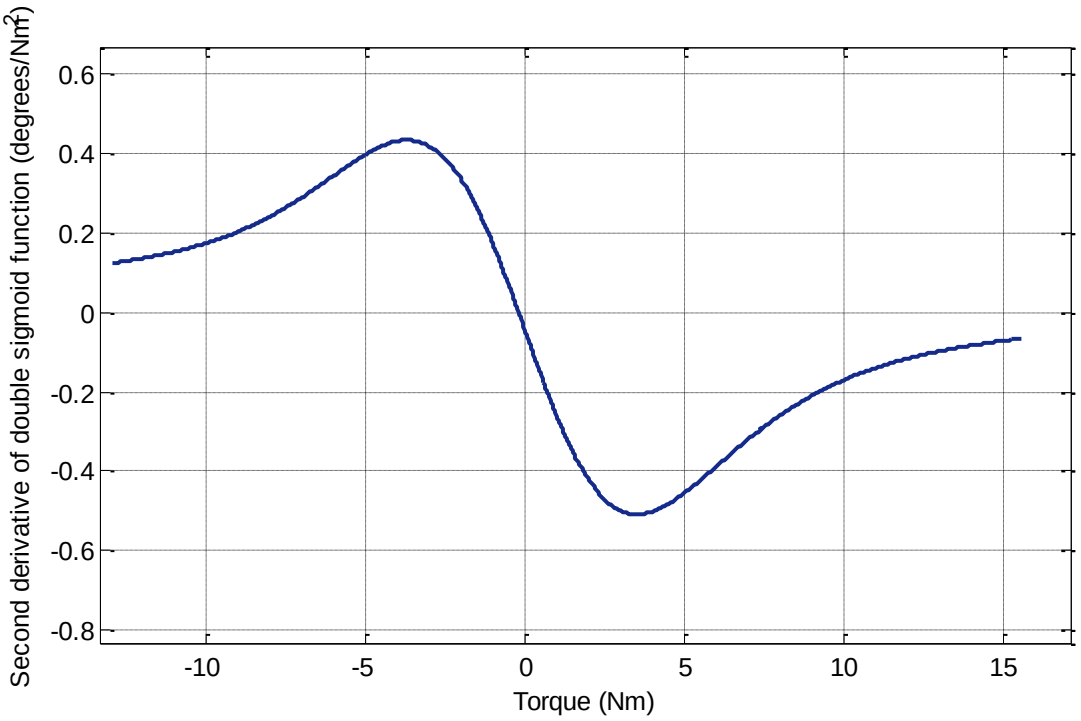

Figure 4.2 Subject 4 Left Lateral bend to Right Lateral bend second derivative curve. Both the maximum and minimum peaks were calculated to determine the neutral zone size.

The goodness of fit R^2 values for each population and loading direction were averaged and shown in Table 4.1. For each population and loading direction, the fitted curves resulted in an average R^2 above 0.9, indicating an excellent fit. Data that fit a linear curve with a $R^2 > 0.7$ and fit the double sigmoid with an $R^2 < 0.7$ were only fit to a linear curve to determine NZ stiffness. Double sigmoid fits and linear fits that both yielded an R^2 below 0.7 were not considered in the remainder of the study. Out of all the data taken, 3 trials (1.4%) were removed from the statistical analysis and 10 trials (4.6%) were only fitted for the neutral zone stiffness.

Table 4.1 Double sigmoid regression Pearson's coefficients' (R^2) are compared between the control and scoliotic populations for each loading direction

	Lateral Bend		**Axial Twist**		**Flexion/Ext**	
	RtoL	*LtoR*	*CWtoCCW*	*CCWtoCW*	*FtoE*	*EtoF*
Control	0.985	0.986	0.918	0.927	0.977	0.976
Scoliosis	0.972	0.973	0.923	0.907	0.960	0.959

The goodness of fit R^2 values inside the neutral zone are compared in Table 4.2. The proposed neutral zone linear regression fit excellently to the double sigmoid shape for each of the loading cases.

Table 4.2 Neutral zone linear regression Pearson's coefficients' (R^2) are compared between the control and scoliotic populations for each loading direction

	Lateral Bend		**Axial Twist**		**Flexion/Ext**	
	RtoL	*LtoR*	*CWtoCCW*	*CCWtoCW*	*FtoE*	*EtoF*
Control	0.997	0.997	0.994	0.982	0.996	0.997
Scoliosis	0.996	0.996	0.985	0.992	0.969	0.964

The goodness of fit R^2 values for both curves outside the neutral zone are compared in Table 4.3. The flexion portion of the fit did not visually resemble a non-linear response. Therefore, Equation 10 was not applied to the flexion portion of the fitted curve. Therefore, a NZ width and ASI could not be calculated for statistical comparison. Only extension β values were used in statistical analyses. The remaining curves outside of the NZ fit well to Equation 9.

Table 4.3 Outside linear region regression Pearson's coefficients' (R^2) are compared between the control and scoliotic populations for each loading direction. Flexion coefficients are absent because no fits were formulated for flexion data.

	Lateral Bend			
	RtoL		*LtoR*	
	Right Side	Left Side	Right Side	Left Side
Control	0.981	0.981	0.977	0.980
Scoliosis	0.984	0.990	0.990	0.975
	Axial Twist			
	CWtoCCW		*CCWtoCW*	
	CW Twist	CCW Twist	CW Twist	CCW Twist
Control	0.977	0.978	0.977	0.979
Scoliosis	0.980	0.984	0.974	0.980
	Flexion/Extension			
	FtoE		*EtoF*	
	Flexion	Extension	Flexion	Extension
Control	-	0.980	-	0.980
Scoliosis	-	0.978	-	0.987

4.2. Comparison of Parameters Between Corresponding Unloading/Loading

The paired sample t-tests between the corresponding unloading/loading directions are shown in Table 4.4. Based on the table, only Lateral_RtoL_ α_left data vs. Lateral_LtoR_ α_left data are significantly different. Therefore, the remaining pairs in Table 4.4 were averaged for subsequent analyses.

Table 4.4 The results of the paired-sample t-test between corresponding loading directions. The text in bold represents a non-significant difference based on an $\alpha = 0.05$ level.

	Paired Differences							
				95% CI of the Difference				
	Mean	Std. Dev	Std. Error Mean	Lower	Upper	t	df	Sig. (2-tailed)
Lateral RtoL NZ Width vs Lateral LtoR NZ Width	-0.568	7.349	1.365	-3.363	2.228	-0.416	28	**0.681**
Lateral RtoL NZStiffness vs Lateral LtoR NZStiffness	-0.002	0.046	0.008	-0.019	0.014	-0.281	30	**0.781**
Lateral RtoL β right vs Lateral LtoR β right	-0.106	0.525	0.098	-0.305	0.094	-1.082	28	**0.288**
Lateral RtoL α right vs Lateral LtoR α right	-0.036	0.641	0.119	-0.280	0.208	-0.302	28	**0.765**
Lateral RtoL β left vs Lateral LtoR β left	0.065	0.217	0.040	-0.018	0.147	1.606	28	**0.120**
Lateral RtoL α left vs Lateral LtoR α left	-0.194	0.347	0.064	-0.326	-0.061	-3.002	28	0.006
Axial CWtoCCW NZ Width vs Axial CCWtoCW NZ Width	-1.595	15.483	2.827	-7.376	4.186	-0.564	29	**0.577**
Axial CWtoCCW NZ Stiffness vs Axial CCWtoCW NZ Stiffness	0.008	0.054	0.010	-0.012	0.028	0.810	29	**0.424**
Axial CWtoCCW β right vs Axial CCWtoCW β right	0.058	0.171	0.031	-0.006	0.122	1.847	29	**0.075**
Axial CWtoCCW α right vs Axial CCWtoCW α right	-0.149	0.458	0.084	-0.320	0.022	-1.782	29	**0.085**
Axial CWtoCCW β left vs Axial CCWtoCW β left	0.072	0.313	0.057	-0.045	0.188	1.253	29	**0.220**
Axial CWtoCCW α left vs Axial CCWtoCW α left	-0.066	0.423	0.077	-0.224	0.092	-0.852	29	**0.401**
FlexExt FtoE NZ Stiffness vs FlexExt EtoF NZ Stiffness	-0.004	0.048	0.009	-0.021	0.014	-0.408	30	**0.686**
FlexExt FtoE β left vs FlexExt EtoF β left	0.000	0.281	0.053	-0.109	0.109	0.006	27	**0.995**
FlexExt FtoE α left vs FlexExt EtoF α left	-0.019	0.469	0.089	-0.201	0.163	-0.213	27	**0.833**

4.3. Interaction Effects and Differences Between Populations

The dependent variable means and corresponding standard deviations are displayed in **Table 4.5**. The marginal averages increased for most of the compared values when comparing the control population to the scoliotic population. Only the lateral neutral zone width and flexion/extension average β decreased when comparing the scoliotic population to the control population.

Table 4.5 The means of the analyzed dependent variables are categorized by anatomical direction and population

Analysis Variable : NZ Width (Degrees)				
Type	**Population**	**N**	**Mean**	**Std Dev**
Lateral Bend	Control	17	33.440	6.429
	Scoliosis	12	22.655	7.450
Axial Twist	Control	17	33.760	7.658
	Scoliosis	13	37.949	6.110
Analysis Variable : NZ Stiffness (Nm/Degree)				
Lateral Bend	Control	17	0.199	0.0590
	Scoliosis	14	0.376	0.148
Axial Twist	Control	17	0.157	0.076
	Scoliosis	13	0.204	0.082
Flexion/ Extension	Control	17	0.181	0.055
	Scoliosis	14	0.289	0.143
Analysis Variable : Average β (1/Degree)				
Lateral Bend	Control	17	0.266	0.078
	Scoliosis	12	0.340	0.183
Axial Twist	Control	17	0.283	0.095
	Scoliosis	11	0.367	0.124
Flexion/ Extension	Control	17	0.316	0.139
	Scoliosis	11	0.308	0.143
Analysis Variable : ASI (Unitless)				
Lateral Bend	Control	17	1.243	0.321
	Scoliosis	12	1.279	0.273
Axial Twist	Control	17	1.311	0.348
	Scoliosis	11	1.335	0.458

The GEE model was applied to the averaged values to determine if there were any interaction effects between the anatomical movements. The interaction between subject population vs. anatomical direction was significant for the NZ width ($p<0.001$), meaning that the

NZ width between subject populations must be further analyzed in each individual anatomical loading direction. Using independent t-tests, the lateral bend NZ width was significantly different between the two subject populations ($p<0.001$) while the axial NZ width was not significantly different between the subject populations ($p = 0.117$)

No interaction was present when comparing NZ stiffness in other anatomical directions (lateral bend vs. flexion/extension, $p = .1894$ and axial twist vs flexion/extension, $p = 0.0613$). However, interaction between subject population and anatomical direction (lateral bend vs. axial twist) was significant ($p=0.0057$). There was significant difference between the populations when comparing the culmination of the NZ stiffnesses ($p<.0001$) Performing an independent t-test analysis on the data, significance difference of NZ stiffness exists between subject populations in lateral bend ($p = 0.001$) and flexion/extension ($p=0.017$). No significant difference in NZ stiffness was apparent in axial twist ($p = 0.110$). Also, a significant negative correlation ($R^2 = -0.499$) was present between the lateral bend NZ width and the NZ stiffness ($p = 0.006$). There was no significant correlation between axial twist NZ and NZ stiffness ($R^2 = .263$, $p = .160$).

The interaction between subject population and all anatomical directions was not significant for the average β parameter (lateral bend vs. axial twist, $p=0.2674$; lateral bend vs. flexion/extension, $p = 0.1334$; and axial twist vs. flexion/extension, $p=0.0613$). The average β parameter used for the flexion/extension trials was considered the β values at extension since flexion β values were not available. Because no interaction effects were apparent, an additive model (no interaction) was then analyzed. With the additive model, anatomical directions individually do not have a significant effect on the average β parameter (lateral bend vs. axial twist, $p=0.4602$ and lateral bend vs flexion/extension, $p=0.5412$). There was no significant

difference in β parameter when comparing the subject populations (p=0.104). Comparing the individual anatomical directions between subject populations, both lateral bend (p=0.167) and axial twist (p=.110) average β values are larger in the scoliotic population but are insignificant.

The interaction between subject population and anatomical direction (lateral bend vs. axial twist) was not significant for ASI (p=0.9449). Again assuming an additive model and excluding the interaction effect in another analysis, anatomical direction (p = 0.5138) and subject population (p=.7428) individually do not have a significant effect on the ASI parameter.

5. DISCUSSION

The purpose of this study was meant to investigate lumbar spine *in vivo* mechanical differences between a scoliotic and control population. The results suggest there are discernable differences between the two tested populations. These differences include the magnitude of the lateral bend NZ width, lateral bend NZ stiffness, and flexion/extension NZ stiffness. Also, the results suggest there are interaction effects when comparing the population type and trial type. This applies to NZ width and NZ stiffness for lateral bend vs. axial twist trials. These results may indicate the mechanical responses to outside forces may be different in scoliotic individuals as compared to a control population.

5.1. Fitted Model

The proposed double sigmoid function in Equation 7 was able to represent most of the subject responses measured in each of the tested trials. This investigation was the first known of its kind to apply the double sigmoid method to define the mechanics of the *in vivo* lumbar spine. The fit from the Smit, van Tunen et al. (2011) paper yielded in an $R^2 > 0.976$ for flexion extension trials. The current study yielded R^2 values (excluding fits with $R^2 < 0.7$) above 0.900, 0.721, and 0.905 for lateral bend, axial twist, and flexion/extension, respectively. The Smit, van Tunen et al. (2011) study only used the third loading cycle to fit the load displacement data, which may have improved the R^2 coefficient for each loaded spine. Multiple loading cycles were used for the double sigmoid fitting regression in the present study. The minor discrepancies in loading rate may have altered the load curves for each pass, creating more error between the fit and the experimental data. As shown in Figure 4.1 and also evident a majority of the other fits, the highest residuals between the fit and experimental were in the near the neutral zone. This section is thought to exhibit the lowest stiffness throughout the load curve. Therefore, the angular displacement sensitivity within the neutral zone will be greater than outside the neutral

zone where the residuals tended to be lower. Even with these possible problems, the average R^2 values indicated an excellent fit.

5.1.1. Neutral Zone Width

The neutral zone was clearly defined by the local extrema of the 2nd derivative of Equation 7. The resulting R^2 values of the linear regression between the proposed NZ limits indicated an extremely good fit for both of the control and scoliotic populations. The scoliotic subjects who could only be fit to a linear curve and not the double sigmoid curve yielded smaller R^2 values as compared to the remaining subjects. This likely occurs because these specific linear regressions were fit to raw data instead of a curve.

The non-apparent NZ limit on the flexion portion of the flexion/extension loading trial may be explained by the physiology of the lumbar spine. Spenciner, Greene et al. (2006) performed an *in vitro* multi-direction loading study on the anterior portion (removal of posterior vertebrae structures) of human cadaver lumbar spinal units. Both the ALL and PLL were left intact. The neutral zone was defined as portion where derivative taken at the end range of motion intersected the displacement axis. The authors separated flexion and extension NZ into two values and found out that the NZ flexion limit was nearly 25% larger than the NZ extension limit. The unequal NZ limits about the neutral position found in the study may explain why the flexion NZ limit may not have been measured in the current study. The authors also found that their NZ width for all of their loading directions ranged from 3.0^o to 4.5^o. Smit, van Tunen et al. (2011), who originally used the double sigmoid function to describe the spinal response, found that NZ width for flexion/extension motions averaged 2.54^o. These neutral zones from both studies are approximately 10 to 11 times smaller than what was computed in this in vivo study. First, both of the previous studies used an *in vitro* setup with a single vertebral joint. Because the present study analyzed the aggregate of the five lumbar spinal joint, the *in vivo* NZ width should

be the superposition of each vertebral joint NZ width. Still, that only accounts for a portion of the discrepancy between the *in vitro* and *in vivo* studies. The *in vitro* studies excluded musculature that may have also affected the size of the neutral zone. To add, the hips and thoracic torso were theoretically fixed in the present study, but perfect fixation was not possible. The culmination of these facts may explain the differences between the present and past *in vitro* studies.

Although the present study was the first to employ the double sigmoid function to the *in vivo* lumbar spine, Kumar and Panjabi (1995) measured the lumbar spine neutral zone in axial twist. The study examined the active range of motion where subjects were asked to assume their neutral positions and then actively rotate to end range of motion for two seconds and then release to return to neutral position. The difference between the initial neutral position and the position to where they stopped moving was considered the neutral zone in the corresponding direction of motion. The same loading cycle was then replicated on the opposite side of rotation. The entire procedure was repeated while the subjects were blind folded. In the third test, the research assistant manually applied torque to the subject's shoulder until the subject asked to stop and was then released to determine the passive neutral zone. In the last test, the research assistant passively torqued subjects in increments based on percentage average axial rotation strength and then released to determine if the neutral zone differs as a result of starting torque.

The mean NZ width from the third test was 6.17^{o} with a standard deviation of 2.67^{o}. The discrepancy of axial twist NZ width between the current study and Kumar and Panjabi (1995) study may be attributed to the experimental setup of both studies. The authors reported that there was no significant difference in NZ width when comparing different starting torques, but also noted a large standard deviation. The authors also found data that support there are a range of

positions in which the spine can stay in equilibrium. The computation of the NZ may not be accurately represented because the inertial parameters have not been minimized. The reported NZ does not directly represent the limit at which the passive structure will offer the least resistance. The NZ more indicates a viscous behavior through the release of internal energy.

5.1.2. Neutral Zone Stiffness

In this present study, the neutral zone stiffness of control subjects was the greatest in the lateral bending, followed by flex/extension, and then by axial twist. Spenciner, Greene et al. (2006) defined flexibility (inverse of stiffness) as the linear portion of the response of a torque displacement plot for *in vitro* intervertebral disc measurements. The author separated the each anatomical movement into separate loading directions (e.g. flexion and extension). Lateral bending exhibited the highest stiffness (2.08 Nm/^{o}), followed by axial rotation (1.96 Nm/^{o}), and then extension (1.82 Nm/^{o}) and flexion (1.54 Nm/^{o}). The *in vivo* lumbar study from McGill, Seguin et al. (1994) did not calculate a linear stiffness, but instead defined stiffness as a function of angular displacement. To compare with the present study, it was assumed that stiffness calculated from McGill, Seguin et al. (1994) at an angular displacement of 2^{o} represented the location of NZ stiffness. At this displacement, the lateral bend had the highest stiffness (0.32 Nm/^{o}), followed by extension (0.17 Nm/^{o}), and then by axial twist (0.13 Nm/^{o}). Another *in vivo* lumbar study used McGill's principle setup to compare lateral side bending stiffness between lower back pain subjects and asymptomatic subjects (Gombatto, Klaesner et al. 2008). The authors found asymptomatic subject stiffness in 0% to 25% angular displacement (approximately the NZ) averaged 0.27 Nm/^{o}. These *in vivo* studies agree well with the present study. The discrepancy between the *in vitro* tests and the *in vivo* tests may be attributed mechanical principles. If the stiffness of a single spinal joint is assumed a spring in series with the adjacent spinal joints, the five lumbar vertebrae should exhibit a lower stiffness as compared to a single

vertebrae, as shown in Equation 12, where only the lumbar joints are considered. However, the *in vivo* trunk will also include stiffness characteristics of some of the thoracic vertebrae.

$$k_{eq} = (\frac{1}{k_{T12-L1}} + \frac{1}{k_{L1-L2}} + \frac{1}{k_{L2-L3}} + \frac{1}{k_{L3-L4}} + \frac{1}{k_{L4-L5}} + \frac{1}{k_{L5-S1}})^{-1} \quad [12]$$

Using the stiffness values from Spenciner, Greene et al. (2006) and assuming all lumbar vertebrae have the same stiffness, the entire lumbar spine stiffness would range from .26 to .35, which is in the range of the described *in vivo* studies and present study.

5.1.3. Outside Neutral Zone

The β parameter computed from Equation 9 determines the rate at which stiffness in the torso increases as the input torque increases. This rate relates to the increased engagement of the passive structures outside of the NZ. The McGill, Seguin et al. (1994) study also used a form Equation 9 to describe the nonlinearity of the asymptomatic *in vivo* spine. The resultant β parameter is compared between genders and anatomical movement in Table 5.1.

Table 5.1 The β parameters from the McGill, Seguin et al. (1994) study including the computed ASI proposed in the current study

	Extension Average	**Axial Twist Average**	**Lateral Bend Average**	**ASI(Axial)**	**ASI (Lateral)**
Males	0.080	0.075	0.110	1.142	1.00
Females	0.080	0.080	0.115	1.28	1.09

The results from the present study are approximately three to five times larger than the study in Table 5.1. First, the study did not consider a linear NZ and the non-linear equation accounts for all of the recorded data. Therefore, the low rate change of stiffness response data near the neutral starting position could contribute in decreasing the β parameter. The ASI's for both the axial and lateral anatomical movements shown in Table 5.1 were closer to the value of 1 as compared to the present study, indicating a near symmetrical stiffness in opposite sides of

anatomical motion (right lateral bend vs. left lateral bend). The asymmetry in the present study may be greater due to the sensitivity of the β parameter. If the data within the NZ was also included in fitting Equation 9, the ASI may have decreased. Also, the asymmetrical stiffness healthy and control subjects have also been witnessed in other studies, suggesting that the stiffness of the spine may be a result of external factors (Gombatto, Norton et al. 2008, Kosmopoulos, Lopez et al. 2012).

5.2. Comparing Population Mechanics

5.2.1. NZ Width

Because of the presence of interactions in NZ width, both anatomical direction type and population were analyzed simultaneously. The average axial twist NZ width for scoliotic subjects was approximately 12% larger than the control population, but statistically insignificant between populations. The possible increase in axial NZ width may actually be due to the degeneration of discs since all of the scoliotic subjects had moderate to severe disc degeneration. Panjabi (1992) stated there are indications, but no conclusive evidence, that relate NZ increase to disc degeneration since the NZ was more sensitive to degeneration as compared to ROM in some analyzed cases. However, the present results also show that the average lateral bend NZ width actually decreases by approximately 33% in the in scoliotic subjects when compared to the control population, contradicting the initial hypothesis that the neutral zone was larger in scoliotic subjects. The discrepancies between the axial twist and lateral bend NZ width may be attributed to the stability mechanisms of the lumbar spine.

The mechanical stability of the spine is maintained by spinal forces from the passive system (intervertebral discs, ligaments, facet joints, etc.) and the active system (muscles). In the neutral position, the passive system does not provide a significant spinal stability as the small muscles of the active system keep the vertebrae upright. The body is able to recognize when the

spine manipulates through movement or a deformity with feedback from the neural system. Panjabi (1992) hypothesized that deformations in ligaments provide more useful neural feedback signals than muscular forces to maintain spinal stability. Stabilizing the spine involves monitoring tissue deformations and selecting appropriate muscles to accommodate for spinal changes to compensate for sudden or gradual changes in the spine. The interplay between the passive, active, and neural system allows the spine to function properly by maintaining a NZ in a stable region.

In the present study, all of the scoliotic subjects showed significant degenerated spines through the combination of intervertebral disc degeneration or facet joint degeneration. For a degraded spine, the neural system may recognize the passive system's inability to provide stability and therefore recruits active system to regain a stable spine. This may cause agonist/antagonist muscle pairs to over activate. The neural system may also detect instability in a scoliotic spine and provide a feedback signal to both the passive and active systems. When the neural system detects that NZ width is too large, the muscular activation may actually reduce the size of the neutral zone as compared to a healthy spine (Wilke, Wolf et al. 1995). Also, the adaptive passive system may form osteophytes to stiffen the spine. Osteophyte growth is also a common result in scoliotic patients as well. Panjabi, Abumi et al. (1989) studied the neutral zones of functional spinal units with simulation of different muscle forces. With increasing muscle forces, ROM increased and the NZ decreased in flexion, ROM and NZ decreased in extension, ROM and NZ unaffected in lateral bend, ROM decreased significantly and NZ decreased insignificantly in axial twist. The authors also simulated injuries to the functional spines including dissection of supraspinous and interspinous ligaments, left medial facetomy, and bilateral medical facetecomites. A 50 N of muscle force restored the NZ or an injured spine

back to the original NZ without injury. This lead to a hypothesis that increased muscle activity in muscle spasm may be an indicator that the body is attempting to stabilize spine. This response may also be present in scoliotic patients from the current study.

Also, facet joints withstand axial loads to help limit intervertebral axial rotation and NZ width of lumbar vertebrae (Panjabi 2003, Thompson, Barker et al. 2003). With the degenerated facet joints in many of the scoliotic subjects, the axial twist NZ may have actually increased and the compensation of the active system could have reduced the NZ back to a perceived healthy state. The axial twist NZ width may not have significantly increased because the active system was engaged. As a result, the lateral bend NZ width was also decreased. Panjabi, Abumi et al. (1989) did not observe the NZ width shrink in lateral bend unlike the present study. However, that study focused on *in vitro* testing which may yield in different results as compared to *in vivo* testing.

The interaction effects between the axial twist NZ width and the lateral bend NZ width may also indicate an altered coupling effect between the lateral bend and axial twist motions. During lateral bend, the movement between the articular surfaces of the facet joints will cause an asymmetric tension within the intertransverse ligaments leading to a rotational movement of vertebrae (Veldhuizen and Scholten 1987). For a scoliotic individual, the spine is manipulated in the fontal plane and the proposed coupling effect also causes axial rotation of the spine. If a motion segment is axially rotated in the local frame, lateral bend of the spine in the global frame will not only cause local lateral rotation, but also local flexion. Also this will cause a lower axial rotational displacement of the vertebral body during lateral bend. For example, if an individual vertebrae is rotated 90^{o}, a global lateral bend will only cause ventral flexion of the individual

vertebrae, and the coupling characteristics between lateral bend and axial twist may not be apparent on the *in vivo* scale.

In scoliosis, the spinous processes in the lumbar spine are rotated towards concave side of the curve viewed from posterior side of the body (Kohno, Ikeuchi et al. 2011). Direction of axial rotation during lateral flexion of scoliotic spine does not differ from healthy spine, but the magnitude of displacement may change (Veldhuizen and Scholten 1987). Also, Legaspi and Edmond (2007) stated that if there is a presence of spinal impairment, the normal coupling pattern is altered. Beuerlein, Raso et al. (2003) examined the individual vertebral axial rotation coupling response of adolescent scoliotic patients. The authors discovered that the axial rotation present in scoliosis was not corrected during the lateral bend even though the scoliotic curve was improved. Coupling may be intact during the formation of scoliosis because axial rotation does occur while the spine laterally deforms. As the scoliotic spine ages, the axial rotations of the spine cause the vertebrae to be fixed in the axially rotated state removing the coupling characteristics.

In the present study, the scoliotic spines have been altered from a healthy position possibly causing the neural system to recognize instability. The active system was recruited to reduce the NZ, which was evidenced in the lateral bend NZ width decrease. The axial twist NZ width in the scoliotic spine did not decrease indicating a possible decoupling characteristic found in the other studies. Also, the degeneration of the facet joints and intervertebral discs may have also reduced the coupling effect since their integrity contributes to the coupling characteristics of the spine (Oxland, Crisco et al. 1992, Rohlmann, Zander et al. 2006). However, it should be noted that the presence of spinal coupling is inconclusive in literature and that the NZ width

differences between the two populations may only be a result of the degenerative differences between the scoliotic and control population (Huijbregts 2004, Legaspi and Edmond 2007).

Although the NZ may have been reduced in the axial twist lateral bend, the progression of scoliosis may not have stabilized since the disease likely progress unless interventions are made. In this case, the body may be only recognizing a mechanical instability and attempting to protect the spine from possible injury through coordination of muscle recruitment (Panjabi 2003). Eventually, this will contribute to more degeneration of the vertebral discs and facet joints. The asymmetric deformity will cause asymmetric loading from muscle activation compensation and therefore asymmetrically degenerates the spine. The body may not be able to recognize the long term effect of reducing the NZ. Because the possible manipulated mechanoreceptors in the ligamentous system, the neuromuscular control system may be receiving corrupted signals and may be providing poor motor control response through overactive muscle activation (Panjabi 2006). Postural stability and motor control issues have also been identified in scoliotic patients (Chen, Wang et al. 1998, Bennett, Abel et al. 2004), which means overcompensated muscle recruitment patterns may be present in scoliotic individuals. The reduction in NZ width may indicate an overcompensation of the active system, accelerating the rate of progression of the scoliotic curve. Further research is necessary to determine if the size of the neutral zone may correlate with the rate of scoliosis progression.

5.2.2. Neutral Zone Stiffness

Overall, the NZ stiffness increased in the scoliotic population as compared to the control population, supporting the second hypothesis. The degenerated spine of the scoliotic subjects may have an effect on the NZ stiffness. *In vitro* and intraoperative studies have found the degeneration of discs have been associated with decreased stiffness in lower levels of degeneration, but increases stiffness in higher levels of degeneration (Fujiwara, Lim et al. 2000,

Brown, Holmes et al. 2002, Zirbel, Stolworthy et al. 2013). Similar results have also been confirmed in finite element studies of the lumbar spine (Rohlmann, Zander et al. 2006, Homminga, Lehr et al. 2013). Zirbel, Stolworthy et al. (2013) postulated that the initial decrease in stiffness may be explained by a fibrocartilage breakdown in annulus fibrosis. The increase in stiffness in more degenerated discs may be a result of the reduced vertical space of the disc. Fujiwara, Lim et al. (2000) also noted that the cartilage degeneration in the facet joints emulated the stiffness properties of the degenerated vertebral discs—decreased stiffness in lower degeneration levels, but increased stiffness in higher degeneration levels. In addition, the author discovered that gender has an influence on spine stiffness. However the role of gender was not investigated in this study due to the low number of male scoliotic patients.

The increased NZ stiffness may also be attributed to the response of the active system through muscle activation. The stiffness of the spine in flexion and extension increases with an increasing axial preload, which occurs during lumbar muscle activation (Tawackoli, Marco et al. 2004). Brown and McGill (2005) simulated increasing force of the rectus abdominis (a muscle that acts on the lumbar torso) and also discovered that increasing muscle force increased the lumbar stiffness. The cross section view of the lumbar torso in Figure 2.5 shows that the surrounding musculature have a larger moment arm as compared to the other passive structures closer to the spine, and therefore active compensation may have a greater effect on the stiffness of the spine. However, lumbar torso muscle activation through EMG was measured at rest in each patient to establish baseline activations. There was no recorded data in the present study to determine if the muscles were more active in the scoliotic population. As a result, active muscular compensation leading to increased spinal stiffness is only a hypothesis.

An interaction effect was also significant in NZ stiffness as the NZ stiffness in lateral bend increases substantially more than the axial twist when comparing the scoliotic population to the control population. Again, this could indicate that the lateral bend and axial twist motions may actually decouple in the scoliotic patient. When comparing the stiffness between populations in each anatomical motion, only the lateral bend NZ stiffness and the flexion/extension NZ stiffness increased significantly for scoliotic patients. The increase of flexion/extension NZ stiffness may be attributed to the presence of osteophytes in the degenerated spine (Fujiwara, Lim et al. 2000).

The presence of a significant correlation between NZ lateral bend stiffness and width may indicate that the passive and active structures attempting to reduce the NZ are also attempting to stiffen the spine. This correlation was applied to both the scoliotic and control populations. This again fortifies the fact that the active system may be overcompensating for the increased NZ width. However, it cannot be determined from the study if the body was attempting to stiffen the spine or reduce the effects of scoliosis. More research is needed to determine the pathological response to scoliosis.

5.2.3. Outside Neutral Zone Stiffness

Average β increased without significance in the axial twist and lateral bend movements, which may be attributed to the low powered subject size in the present study. Also, scoliotic subject variability may have attributed to the large standard deviation in the population, specifically in lateral bend.

Parameter β represents that rate at which stiffness of the spine increases as torque applied also increases. The change to a rapidly increasing stiffness outside of the neutral zone may be due to the tension properties of the spinal ligaments. The collagen structure of the ligaments allows little resistance at lower strains but will become significantly stiffer at higher strains

(Hukins and Meakin 2000). Also, the ligaments can still withstand significant load even after damage. The facet joints provide the most amount of resistance in torsion because the movement causes the bony facets to impinge. An increasing β suggests a more nonlinear change in stiffness of the spine even though the ligaments and facets may have been compromised. However, Rohlmann, Zander et al. (2006) completed a finite study and found that increased disc degeneration causes nonlinear force-displacement curves of healthy discs become more linear. The Rohlmann study was void of any musculature that may have actually increased the nonlinearity found in the current study.

While the average β did increase in both the axial twist and lateral bend cases, the mean extension β decreased slightly in scoliotic patients, which contradicts that the muscles and osteophytes are stiffening the spine. However, facet joints, which were moderately to severely degenerated in the study, are important in restricting extension movements (Sharma, Langrana et al. 1995). Although the spine may have stiffened in other two anatomical planes of motion, the active and passive system responses may not have accommodated for the degenerated facet joints.

No significant differences in asymmetrical stiffness between the two subject populations were found in the current study, contradicting the third hypothesis. Although scoliotic subject exhibited ASI values greater than one, similar asymmetrical stiffness characteristics were apparent in the control population. However, intraoperative testing (Reutlinger, Hasler et al. 2012) and radiographic mathematical models(Lafon, Lafage et al. 2010) have shown that asymmetrical lateral bend stiffness characteristics are apparent in scoliotic individuals. Lafon, Lafage et al. (2010) used radiographic data of scoliotic subjects in neutral and side lateral bend. With optimization techniques, the authors calculated the distribution of stiffness across the spine

among the passive structures. They found that the asymmetry was apparent in each vertebral segment in a scoliotic patient, meaning the asymmetrical stiffness should be apparent in the present study. However, the mathematical model did not include the musculature of the scoliotic patient. The inclusion of muscles in the present study may actually reduce the ASI to that of the control population.

5.3. Limitations

5.3.1. Apparatus

The apparatus used in this study was meant to comfortably fit human subjects. To achieve this, the lateral bend and flexion/extension apparatus needed to accommodate both populations. Theoretically, the hips and lower extremities are fixed to the global frame but these body parts could move minimally in the apparatus. However, the inclusion of the reference motion sensor on the hips accounted for the small movement of the hips. This still assumes the structures of the hip are fixed rigidly when in actuality there may be movement. Because the lumbar torso was modeled as a lumped parameter system, it was impossible to tell if movement was exclusive to the thoraco-lumbar vertebrae. Stiffness characteristics may have also included the thoracic spine.

In the flexion-extension trials, scoliotic subjects were asked to lie on their side that was the most comfortable. However, this did not control if the concave or convex side of the scoliotic spine was facing upwards. Future research should ensure orientation of scoliotic curve remains consistent for each scoliotic subject in the flexion/extension trials. Also, the flexion NZ limit was not visually apparent and a NZ could not be defined for the flexion/extension data. More testing is necessary to determine what ROM limit should be used to properly record the flexion NZ limit.

In the axial twist setup, torso inclination was visually confirmed along with the subjects' response to ensure a vertical torso during testing, but no instrumentation was used to determine torso inclination. Recorded axial twist stiffness may have been altered due to slightly different lumbar flexion and extension postures causing disengagement/engagement of the facet joints. (Drake and Callaghan 2008). Also as subjects sat on the rotating seat, the induced axial torque may have also induced torque in another anatomical direction because subjects may not have directly aligned their vertebral column in the center of rotation.

Since the research assistant was directly applying the torque to the subject, the velocity and acceleration parameters were limited to human control instead of an automated process. Although the metronome provided time increments for constant velocity, small movements in the apparatus that may have altered the mechanical response were not accounted for. However, the human controlled apparatus allowed versatility in the testing procedure in case of an emergency. Additionally, the motion sensors were fastened to the subject's clothing during testing instead of the skin, allowing possible unwanted mobility of the sensors on the skin. However, the slow angular velocity reduced the chance that inertial effects may have moved the sensor during testing.

5.3.2. Model

Modeling the lumbar spine and torso response as a linear system provides a simple method to quantify the lumbar spine mechanics, but may obscure the differences in lumbar torso mechanics. Generally, a lumped parameter system accounts for the inertial properties of the human subject, but both the rotational acceleration and angular velocity terms were ignored in this study to simplify the analysis further. With the proposed constant angular velocity, the rotational acceleration was assumed to equal zero. At the end range of motion, the changes in direction cause an angular acceleration that was not accounted for, causing a possible false load

cell reading. Because of a low angular velocity, viscous effects were assumed to be negligible as compared to the stiffness effects. The non-zero constant velocity in the study could have also increased the recorded force from the load cell due to internal human body viscous effects. Although these acceleration and velocity effects were deemed negligible, their effect on the loading response should be investigated in future studies.

Because of the viscoelastic and pseudoelastic properties of soft tissues, the loading rate will have an effect on the stiffness characteristics of the spine (Fung 1984). Spenciner, Greene et al. (2006) noticed that the average NZ increased while the stiffness stayed constant for each subsequent test. Goertzen, Lane et al. (2004) compared the effect of step vs. continuous loading rates on cervical porcine cervical spine specimens and found that step loading rates caused the largest NZ, eluding to a probable viscoelastic effect. Other viscoelastic and pseudoelastic models may need to be employed in future studies to explain the mechanical characteristics of the lumbar spine.

Fitting the double sigmoid function to the proposed data allowed for asymmetrical differences to opposite sides of the neutral position. However, the least squares method of curve fitting lead to various solutions, rendering the biomechanical parameters of the double sigmoid function useless to compare between populations. Also, some of the subjects were unable to withstand the $\pm 30^{o}$ ROM originally proposed and the double sigmoid function may not have encapsulated the true torque angular displacement data. Also, the second derivate of the double sigmoid curve sometimes included more than two local extrema, occluding the true limits of the NZ. Smit, van Tunen et al. (2011) proposed this may occur as a result of impingement or tissue damage that may be apparent in a normal and scoliotic adult. If the second derivative included

multiple maximums or minimums, visual inspection confirmed the true limits of the neutral zone.

The model was also not able to capture the asymmetries in NZ width. For some subjects, the NZ limits were on the same side of the zero load axis, which is theoretically impossible. During testing, the neutral position was sensitive since the resistance in the NZ was minimized. Therefore, the recorded neutral position in testing may not have been actual neutral position. Future studies should develop methods to determine the true neutral position within the NZ.

5.3.3. Subject Populations

The amount of recruited subjects was below the proposed power study. Although there were differences between subject populations, an increase in both the scoliotic and control population could have found more significant differences in biomechanical parameters between the two tested populations. Also, scoliosis is a complex disease that may be unique among patients. In order to determine if there is a correlation between Cobb angle, apex level, lordosis angle, etc., more lumbar scoliotic subjects would need to be tested. Some of the data in scoliotic patients did not reveal a NZ because a reduction in perceived ROM. More pre-tests for ROM limits should be completed prior to the data acquisition phase to ensure the scoliotic patients can partake in the experiment.

All of the scoliotic subjects were aged over 45 years. Matching the tested population was difficult as a majority control subjects were recruited subjects from a college aged population. However, an *in vitro* study has shown that increasing age does not significantly affect the stiffness characteristics of the lumbar vertebrae (Nachemson, Schultz et al. 1979). Furthermore, age may have an inverse effect on the stiffness characteristics since a study found there was a weak ($R^2 = 0.23$) negative correlation between age and the elastic modulus of the spinal ligaments (Iida, Abumi et al. 2002). The present study found that the older population actually

had stiffer spines. The stiffness of scoliotic subjects recorded in this study may have actually been attenuated compared to the younger control population because their passive structures may have provided less resistance. Also, the scoliotic population consisted more of females (79%) as compared to the control population (47%). Studies have shown that females exhibit decreased spine stiffness and resistance as compared to a male population (Nachemson, Schultz et al. 1979, McGill, Jones et al. 1994). The increased proportion of female scoliotic subjects may have resulted in a decreased stiffness in the scoliotic population as compared by a more male dominated control group. Although significant differences between populations existed, factoring out both the age and gender discrepancy may reveal more significant differences between the two compared populations.

5.4. Future Steps

The lumped parameter model will be expanded to include the acceleration and velocity parameters to validate the model. Another study had also fit a viscoelastic lumped parameter system to determine the anterior-posterior movement of the *in vivo* lumbar spine (Nicholson, Maher et al. 2001). The authors found that the *in vivo* spine fit well to their model. Future studies will also employ viscoelastic models to determine how the passive lumbar spine can be best represented.

More studies will be needed to determine if results from the lump parameter models can help engineers and scientists understand the progression of the disease. Panjabi (2003) developed checklist that accounts for biomechanics, neurologic damage, and anticipated loading on the spine. A similar checklist may also be developed to accompany the ways to classify scoliosis and understand it as it progresses. Also, future research should be developed to determine if this apparatus can be used to clinically test for risk analysis of scoliosis progression.

6. CONCLUSION

The current study employed a lumped parameter system to measure the neutral zone width, neutral zone stiffness, overall outside neutral zone stiffness, and outside neutral zone stiffness asymmetries for flexion/extension, lateral bend, and axial twist in lumbar degenerative scoliotic subjects and control subjects. The model was able to accurately represent the mechanical response of the lumbar spine and provide a comparison tool between the subject populations. The results suggested scoliotic subjects exhibit a smaller lateral bend NZ width but a similar axial twist NZ width as compared to a control population. This contradicts the initial hypothesis that the overall NZ width would be larger in scoliotic subjects. The initial hypothesis only considered the degenerated spine. However, the response of the active and passive system must be taken into account as the body attempts to compensate for the changes in the spine. The overall stiffness within the NZ increased significantly while stiffness outside the NZ increased insignificantly. Asymmetries between the scoliotic group and control group were not significantly different, disproving the third hypothesis. Although an asymmetrical deformation is present, the scoliotic body still replicates the asymmetries found in control subjects. Also, the results suggest there are interaction effects when comparing the population type and trial type. This applies to NZ width and NZ stiffness for lateral bend vs. axial twist trials. The interaction effects indicate that the coupling effects found in the control population may actually be altered in the scoliotic population.

The present study was the first investigation to quantify the *in vivo* neutral zone and related mechanics of the scoliotic lumbar spine. Future research is needed to determine if the model can provide useful mechanical knowledge for therapy or surgical decisions.

APPENDIX

A.1. Preliminary Results

The following lateral bend data were taken from a single subject with a healthy lumbar spine to determine the validity of the proposed techniques. Preliminary data has only utilized Eularian angles from a single sensor with repeatable results.

The first test intended to move the subject at a constant 30^{o}/s to try to replicate the proposed double sigmoid shape. The end ROM velocity was reversed almost immediately to reduce the effects of transient changes in the velocity. At this high speed, the quick change in velocity induced a force caused by the inertial properties instead of the stiffness characteristics of the lumbar spine. Also, the research assistant could not account for the non-linearity stiffness of the spine through the quick change in deflection, causing a non-constant angular velocity. The angular deflection is plotted against the induced force in Figure A**.1**. The outputted angular displacement drifted approximately $+10^{o}$ during the trial, which may indicate the large spread of data in the graph. The shape of the hysteresis is not apparent, however. Two more tests were completed at 15^{o}/s and 7.5^{o}/s in an effort to reduce the inertial effects and allow the research assistant to account the changing stiffness of the spine. The resultant angular deflection vs. force graphs for the 15^{o}/s and 7.5^{o}/s are plotted in Figure A**.2** and Figure A**.3**, respectively. During these trials, the angular shift due to the magnetic force was not apparent compared to the 30^{o}/s trial. The Figure A**.2** graph showing the 15^{o}/s trial resembled the double sigmoid shape desired, but there was still not evident hysteresis loop even though the drift was minimized. The Figure A**.3** graph clearly displays the hysteresis loop and more closely resembles the double sigmoid shape.

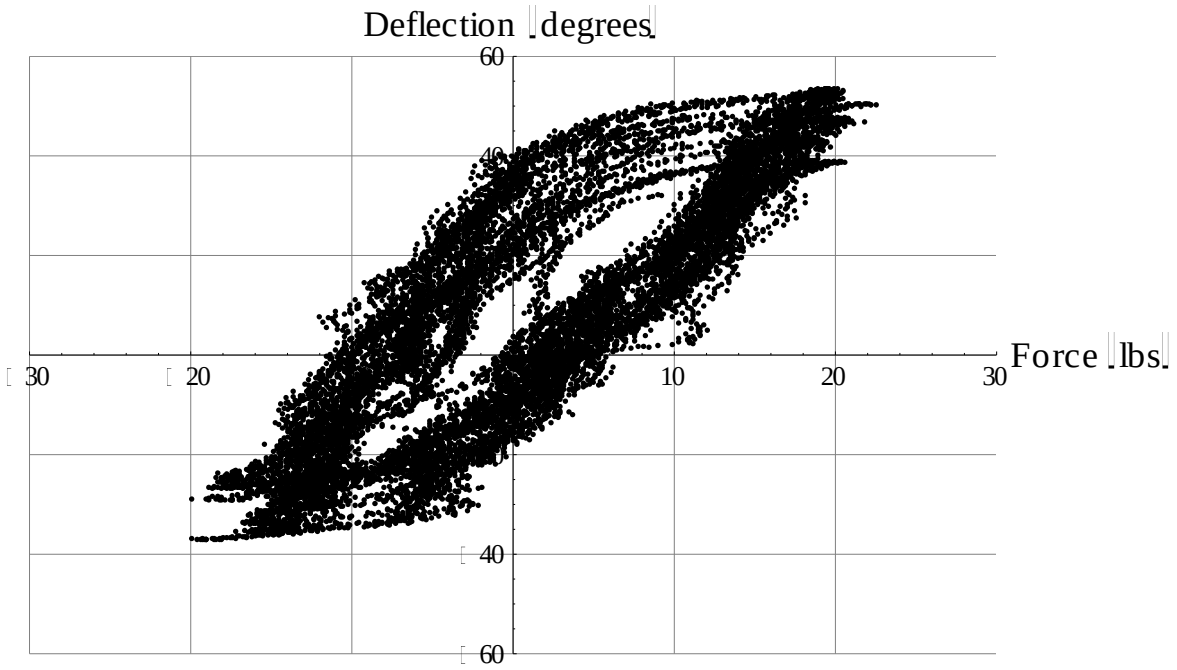

Figure A.1 Lateral bending Testing at 30°/s. 15 cycles with considerable angle drift.

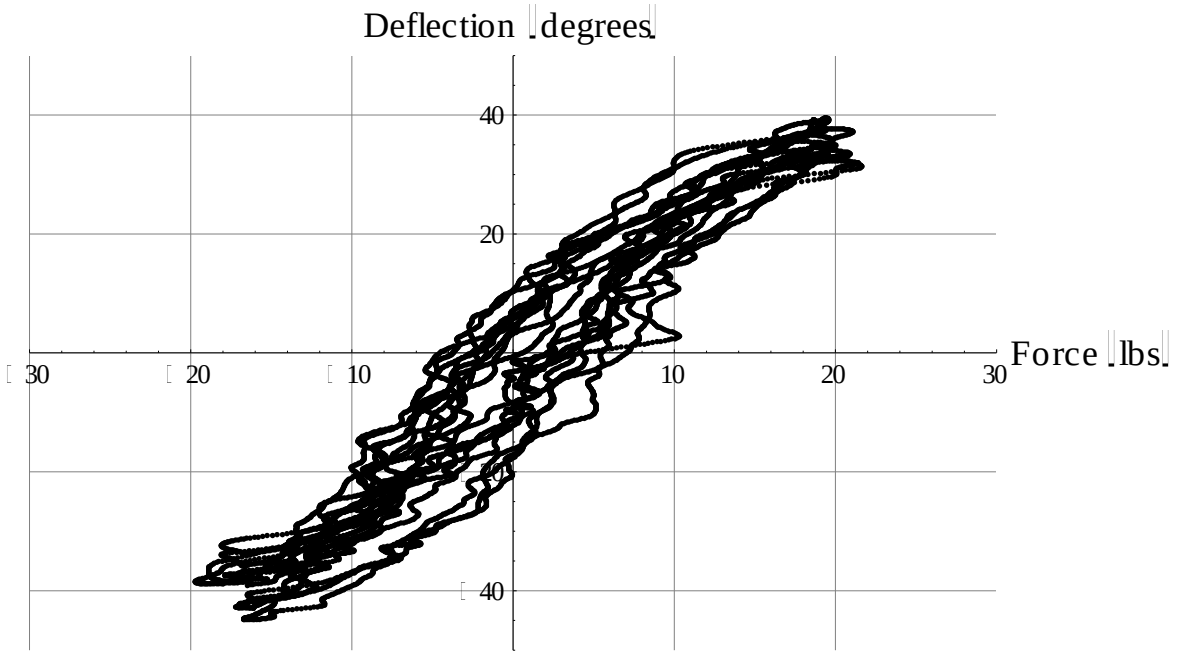

Figure A.2 Lateral bending Testing at 15°/s. 8 cycles.

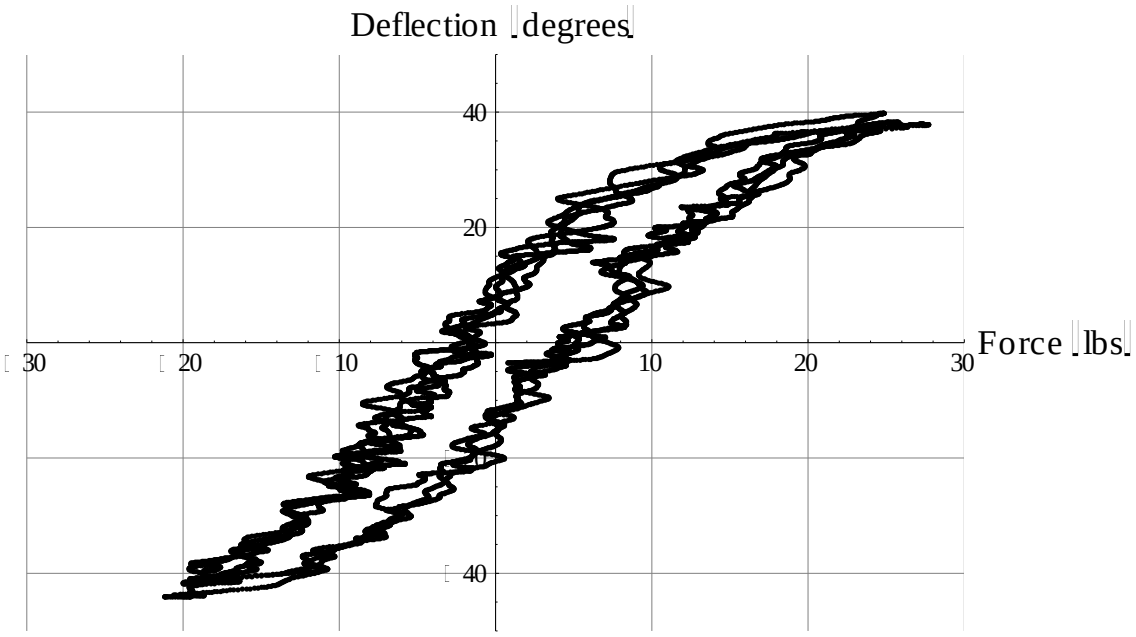

Figure A.3 Lateral bending Testing at 7.5°/s. 4 cycles.

Using the data from the 7.5°/s trial, the double sigmoid curve was fitted to both the top and bottom portions of the hysteresis curve. The resultant curves are displayed in Figure A**.4**.

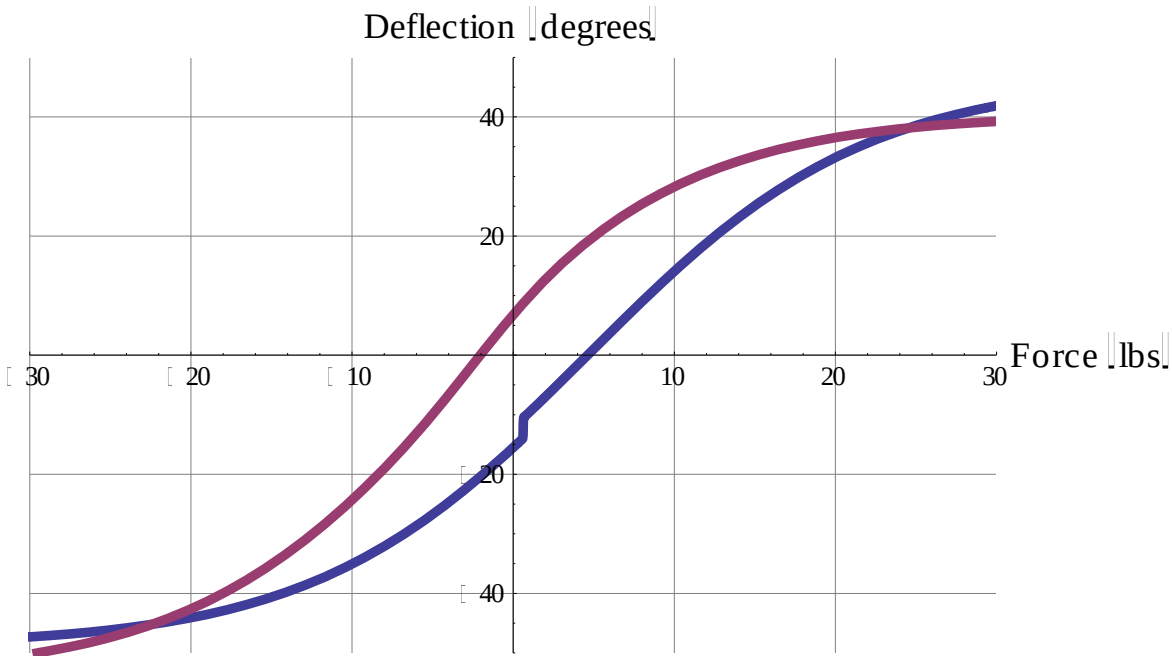

Figure A.4 Both the top and bottom portions fitted to the double sigmoid function. The vertical line in the blue curve could be due to the numerical instability in the FindFit function from Mathematica.

REFERENCES

Aebi, M. (2005). "The adult scoliosis." European Spine Journal **14**(10): 925-948.

Beach, T. A., R. J. Parkinson, J. P. Stothart and J. P. Callaghan (2005). "Effects of prolonged sitting on the passive flexion stiffness of the in vivo lumbar spine." Spine J **5**(2): 145-154.

Bennett, B. C., M. F. Abel and K. P. Granata (2004). "Seated postural control in adolescents with idiopathic scoliosis." Spine (Phila Pa 1976) **29**(20): E449-454.

Beuerlein, M. J., V. J. Raso, D. L. Hill, M. J. Moreau and J. K. Mahood (2003). "Changes in alignment of the scoliotic spine in response to lateral bending." Spine (Phila Pa 1976) **28**(7): 693-698.

Bisschop, A., I. Kingma, R. L. Bleys, C. P. Paul, A. J. van der Veen, B. J. van Royen and J. H. van Dieen (2013). "Effects of repetitive movement on range of motion and stiffness around the neutral orientation of the human lumbar spine." J Biomech **46**(1): 187-191.

Brodeur, R. and L. DelRe (1999). "Stiffness of the Thoraco-LumbarSpine for Subjects With and WithoutLow Back Pain." Journal of the Neuromusculoskeletal System **7**(4): 127-133.

Brown, M. D., D. C. Holmes and A. D. Heiner (2002). "Measurement of cadaver lumbar spine motion segment stiffness." Spine (Phila Pa 1976) **27**(9): 918-922.

Brown, S. H., D. E. Gregory, J. A. Carr, S. R. Ward, K. Masuda and R. L. Lieber (2011). "ISSLS prize winner: Adaptations to the multifidus muscle in response to experimentally induced intervertebral disc degeneration." Spine (Phila Pa 1976) **36**(21): 1728-1736.

Brown, S. H. and S. M. McGill (2005). "Muscle force-stiffness characteristics influence joint stability: a spine example." Clin Biomech (Bristol, Avon) **20**(9): 917-922.

Chamie, J. (2002). World Population Ageing 1950-2050. J. Chamie, United Nations, New York, NY. Dept. of Economic and Social Affairs.**:** 15-22.

Chen, P. Q., J. L. Wang, Y. H. Tsuang, T. L. Liao, P. I. Huang and Y. S. Hang (1998). "The postural stability control and gait pattern of idiopathic scoliosis adolescents." Clin Biomech (Bristol, Avon) **13**(1 Suppl 1): S52-s58.

Cobb, J. B. (1948). Outline for the study of scoliosis. Instructional course lectures, American Academy of Orthopaedic Surgeons, Ann Arbor, MI**:** 261–275.

Drake, J. D. M. and J. P. Callaghan (2008). "Do flexion/extension postures affect the in vivo passive lumbar spine response to applied axial twist moments?" Clinical Biomechanics **23**(5): 510-519.

Duance, V. C., J. K. Crean, T. J. Sims, N. Avery, S. Smith, J. Menage, S. M. Eisenstein and S. Roberts (1998). "Changes in collagen cross-linking in degenerative disc disease and scoliosis." Spine (Phila Pa 1976) **23**(23): 2545-2551.

Eberlein, R., G. A. Holzapfel and M. Fröhlich (2004). "Multi-segment FEA of the human lumbar spine including the heterogeneity of the annulus fibrosus." Computational Mechanics **34**(2): 147-163.

Faldini, C., A. Di Martino, M. De Fine, M. T. Miscione, C. Calamelli, A. Mazzotti and F. Perna (2013). "Current classification systems for adult degenerative scoliosis." Musculoskelet Surg **97**(1): 1-8.

Friden, J. and R. L. Lieber (2003). "Spastic muscle cells are shorter and stiffer than normal cells." Muscle Nerve **27**(2): 157-164.

Fujiwara, A., T. H. Lim, H. S. An, N. Tanaka, C. H. Jeon, G. B. Andersson and V. M. Haughton (2000). "The effect of disc degeneration and facet joint osteoarthritis on the segmental flexibility of the lumbar spine." Spine (Phila Pa 1976) **25**(23): 3036-3044.

Fung, Y. (1984). "Structure and stress-strain relationship of soft tissues." American Zoologist **24**(1): 13-22.

Glassman, S. D., L. Y. Carreon, C. I. Shaffrey, D. W. Polly, S. L. Ondra, S. H. Berven and K. H. Bridwell (2010). "The costs and benefits of nonoperative management for adult scoliosis." Spine (Phila Pa 1976) **35**(5): 578-582.

Goertzen, D. J., C. Lane and T. R. Oxland (2004). "Neutral zone and range of motion in the spine are greater with stepwise loading than with a continuous loading protocol. An in vitro porcine investigation." J Biomech **37**(2): 257-261.

Gombatto, S. P., J. W. Klaesner, B. J. Norton, S. D. Minor and L. R. Van Dillen (2008). "Validity and reliability of a system to measure passive tissue characteristics of the lumbar region during trunk lateral bending in people with and people without low back pain." J Rehabil Res Dev **45**(9): 1415-1429.

Gombatto, S. P., B. J. Norton, S. A. Scholtes and L. R. Van Dillen (2008). "Differences in symmetry of lumbar region passive tissue characteristics between people with and people without low back pain." Clin Biomech (Bristol, Avon) **23**(8): 986-995.

Gray, H. (1918). Anatomy of the Human Body. Philadelphia, Lea & Febiger.

Grivas, T. B. (2010). "Differential diagnosis of back pain in adult operated scoliosis patients." Scoliosis **5**(Suppl 1): O45.

Grubb, S. A. and H. J. Lipscomb (1992). "Diagnostic findings in painful adult scoliosis." Spine **17**(5): 518-527.

Grubb, S. A., H. J. Lipscomb and R. W. Coonrad (1988). "Degenerative adult onset scoliosis." Spine **13**(3): 241-245.

Homminga, J., A. M. Lehr, G. J. Meijer, M. M. Janssen, T. P. Schlosser, G. J. Verkerke and R. M. Castelein (2013). "Posteriorly directed shear loads and disc degeneration affect the torsional stiffness of spinal motion segments: a biomechanical modeling study." Spine (Phila Pa 1976) **38**(21): E1313-1319.

Howarth, S. J., K. M. Gallagher and J. P. Callaghan (2013). "Postural influence on the neutral zone of the porcine cervical spine under anterior-posterior shear load." Med Eng Phys **35**(7): 910-918.

Huijbregts, P. (2004). "Lumbar spine coupled motions: A literature review with clinical implications." Orthopaedic Division Review.

Hukins, D. W. L. and J. R. Meakin (2000). "Relationship Between Structure and Mechanical Function of the Tissues of the Intervertebral Joint." American Zoologist **40**(1): 42-052.

Ialenti, M., B. Lonner, P. Penn, P. Ricart-Hoffiz, L. Wyndsor, F. Schwab and T. Errico (2010). Hospital Cost Analysis of Adult Scoliosis Surgery in 120 Consecutive Cases. 45th Annual SRS Meeting, Kyoto, Japan

Iida, T., K. Abumi, Y. Kotani and K. Kaneda (2002). "Effects of aging and spinal degeneration on mechanical properties of lumbar supraspinous and interspinous ligaments." Spine J **2**(2): 95-100.

Jackson, R. P., E. H. Simmons and D. STRIPINIS (1983). "Incidence and severity of back pain in adult idiopathic scoliosis." Spine **8**(7): 749-756.

Kim, H., C.-K. Lee, J. S. Yeom, J. H. Lee, J. H. Cho, S. I. Shin, H.-J. Lee and B.-S. Chang (2013). "Asymmetry of the cross-sectional area of paravertebral and psoas muscle in patients with degenerative scoliosis." European Spine Journal: 1-7.

Kobayashi, T., Y. Atsuta, M. Takemitsu, T. Matsuno and N. Takeda (2006). "A prospective study of de novo scoliosis in a community based cohort." Spine **31**(2): 178-182.

Kohno, S., M. Ikeuchi, S. Taniguchi, R. Takemasa, H. Yamamoto and T. Tani (2011). "Factors predicting progression in early degenerative lumbar scoliosis." Journal of Orthopaedic Surgery **19**(2).

Kosmopoulos, V., J.-A. Lopez, J. McCain and S. Kumar (2012). "In Vivo Passive AxialRotational Stiffness of the Thoracolumbar Spine."

Kumar, S. and M. M. Panjabi (1995). "In vivo axial rotations and neutral zones of the thoracolumbar spine." J Spinal Disord **8**(4): 253-263.

Kurutz, M. (2010). Finite Element Modelling of Human Lumbar Spine. Finite Element Analysis. D. Moratal, InTech.

Lafage, V., P. Leborgne, A. Mitulescu, J. Dubousset, F. Lavaste and W. Skalli (2002). "Comparison of mechanical behaviour of normal and scoliotic vertebral segment: a preliminary numerical approach." Studies in health technology and informatics: 340-344.

Lafon, Y., V. Lafage, J.-P. Steib, J. Dubousset and W. Skalli (2010). "In vivo distribution of spinal intervertebral stiffness based on clinical flexibility tests." Spine **35**(2): 186-193.

Legaspi, O. and S. L. Edmond (2007). "Does the evidence support the existence of lumbar spine coupled motion? A critical review of the literature." J Orthop Sports Phys Ther **37**(4): 169-178.

Little, J. P. and C. J. Adam (2009). "The effect of soft tissue properties on spinal flexibility in scoliosis: biomechanical simulation of fulcrum bending." Spine **34**(2): E76-E82.

Little, J. S. and P. S. Khalsa (2005). "Human lumbar spine creep during cyclic and static flexion: creep rate, biomechanics, and facet joint capsule strain." Ann Biomed Eng **33**(3): 391-401.

Lowe, T., S. H. Berven, F. J. Schwab and K. H. Bridwell (2006). "The SRS classification for adult spinal deformity: building on the King/Moe and Lenke classification systems." Spine (Phila Pa 1976) **31**(19 Suppl): S119-125.

Lupparelli, S., E. Pola, L. Pitta, O. Mazza, V. De Santis and L. Aulisa (2002). "Biomechanical factors affecting progression of structural scoliotic curves of the spine." Studies in health technology and informatics **91**: 81.

Mannion, A. F., M. Meier, D. Grob and M. Muntener (1998). "Paraspinal muscle fibre type alterations associated with scoliosis: an old problem revisited with new evidence." Eur Spine J **7**(4): 289-293.

Marty-Poumarat, C., L. Scattin, M. Marpeau, C. G. de Loubresse and P. Aegerter (2007). "Natural history of progressive adult scoliosis." Spine **32**(11): 1227-1234.

McGill, S., J. Seguin and G. Bennett (1994). "Passive stiffness of the lumbar torso in flexion, extension, lateral bending, and axial rotation. Effect of belt wearing and breath holding." Spine (Phila Pa 1976) **19**(6): 696-704.

McGill, S. M. and S. Brown (1992). "Creep response of the lumbar spine to prolonged full flexion." Clin Biomech (Bristol, Avon) **7**(1): 43-46.

McGill, S. M., K. Jones, G. Bennett and P. J. Bishop (1994). "Passive stiffness of the human neck in flexion, extension, and lateral bending." Clin Biomech (Bristol, Avon) **9**(3): 193-198.

Mimura, M., M. Panjabi, T. Oxland, J. Crisco, I. Yamamoto and A. Vasavada (1994). "Disc degeneration affects the multidirectional flexibility of the lumbar spine." Spine **19**(12): 1371-1380.

Moramarco, V., A. Pérez del Palomar, C. Pappalettere and M. Doblaré (2010). "An accurate validation of a computational model of a human lumbosacral segment." Journal of Biomechanics **43**(2): 334-342.

Nachemson, A. L., A. B. Schultz and M. H. Berkson (1979). "Mechanical properties of human lumbar spine motion segments. Influence of age, sex, disc level, and degeneration." Spine (Phila Pa 1976) **4**(1): 1-8.

Nicholson, L., C. Maher, R. Adams and N. Phan-Thien (2001). "Stiffness properties of the human lumbar spine: a lumped parameter model." Clin Biomech (Bristol, Avon) **16**(4): 285-292.

O'Brien, J. (2010). "Living with scoliosis: an adult perspective." Scoliosis **5**(Suppl 1): O43.

Oxland, T. R., J. J. Crisco, 3rd, M. M. Panjabi and I. Yamamoto (1992). "The effect of injury on rotational coupling at the lumbosacral joint. A biomechanical investigation." Spine (Phila Pa 1976) **17**(1): 74-80.

Panjabi, M., K. Abumi, J. Duranceau and T. Oxland (1989). "Spinal stability and intersegmental muscle forces. A biomechanical model." Spine (Phila Pa 1976) **14**(2): 194-200.

Panjabi, M. M. (1992). "The stabilizing system of the spine. Part I. Function, dysfunction, adaptation, and enhancement." J Spinal Disord **5**(4): 383-389; discussion 397.

Panjabi, M. M. (1992). "The stabilizing system of the spine. Part II. Neutral zone and instability hypothesis." Journal of spinal disorders & techniques **5**(4): 390-397.

Panjabi, M. M. (2003). "Clinical spinal instability and low back pain." J Electromyogr Kinesiol **13**(4): 371-379.

Panjabi, M. M. (2006). "A hypothesis of chronic back pain: ligament subfailure injuries lead to muscle control dysfunction." Eur Spine J **15**(5): 668-676.

Panjabi, M. M., V. K. Goel and K. Takata (1982). "Physiologic Strains in the Lumbar Spinal Ligaments: An In VitroBiomechanical Study." Spine **7**(3): 192-203.

Petit, Y., C. E. Aubin and H. Labelle (2004). "Patient-specific mechanical properties of a flexible multi-body model of the scoliotic spine." Med Biol Eng Comput **42**(1): 55-60.

Pintar, F. A., N. Yoganandan, T. Myers, A. Elhagediab and A. Sances, Jr. (1992). "Biomechanical properties of human lumbar spine ligaments." J Biomech **25**(11): 1351-1356.

Ploumis, A., E. E. Transfledt and F. Denis (2007). "Degenerative lumbar scoliosis associated with spinal stenosis." The Spine Journal **7**(4): 428-436.

Prado, L. G., I. Makarenko, C. Andresen, M. Kruger, C. A. Opitz and W. A. Linke (2005). "Isoform diversity of giant proteins in relation to passive and active contractile properties of rabbit skeletal muscles." J Gen Physiol **126**(5): 461-480.

Reutlinger, C., C. Hasler, K. Scheffler and P. Buchler (2012). "Intraoperative determination of the load-displacement behavior of scoliotic spinal motion segments: preliminary clinical results." Eur Spine J **21 Suppl 6**: S860-867.

Rohlmann, A., T. Zander, H. Schmidt, H. J. Wilke and G. Bergmann (2006). "Analysis of the influence of disc degeneration on the mechanical behaviour of a lumbar motion segment using the finite element method." J Biomech **39**(13): 2484-2490.

Ruberté, L. M., R. N. Natarajan and G. B. J. Andersson (2009). "Influence of single-level lumbar degenerative disc disease on the behavior of the adjacent segments—A finite element model study." Journal of Biomechanics **42**(3): 341-348.

Ruiz Santiago, F., P. P. Alcazar Romero, E. Lopez Machado and M. A. Garcia Espona (1997). "Calcification of lumbar ligamentum flavum and facet joints capsule." Spine (Phila Pa 1976) **22**(15): 1730-1734; discussion 1734-1735.

Scannell, J. P. and S. M. McGill (2003). "Lumbar posture--should it, and can it, be modified? A study of passive tissue stiffness and lumbar position during activities of daily living." Phys Ther **83**(10): 907-917.

Schendel, M. J., K. B. Wood, G. R. Buttermann, J. L. Lewis and J. W. Ogilvie (1993). "Experimental measurement of ligament force, facet force, and segment motion in the human lumbar spine." J Biomech **26**(4-5): 427-438.

Schwab, F., A. B. el-Fegoun, L. Gamez, H. Goodman and J.-P. Farcy (2005). "A lumbar classification of scoliosis in the adult patient: preliminary approach." Spine **30**(14): 1670-1673.

Schwab, F., J. P. Farcy, K. Bridwell, S. Berven, S. Glassman, J. Harrast and W. Horton (2006). "A clinical impact classification of scoliosis in the adult." Spine (Phila Pa 1976) **31**(18): 2109-2114.

Schwab, F. J., V. A. Smith, M. Biserni, L. Gamez, J.-P. C. Farcy and M. Pagala (2002). "Adult scoliosis: a quantitative radiographic and clinical analysis." Spine **27**(4): 387-392.

Seo, J.-Y., K.-Y. Ha, T.-H. Hwang, K.-W. Kim and Y.-H. Kim (2011). "Risk of progression of degenerative lumbar scoliosis: Clinical article." Journal of Neurosurgery: Spine **15**(5): 558-566.

Shafaq, N., A. Suzuki, A. Matsumura, H. Terai, H. Toyoda, H. Yasuda, M. Ibrahim and H. Nakamura (2012). "Asymmetric degeneration of paravertebral muscles in patients with degenerative lumbar scoliosis." Spine **37**(16): 1398-1406.

Sharma, M., N. A. Langrana and J. Rodriguez (1995). "Role of ligaments and facets in lumbar spinal stability." Spine (Phila Pa 1976) **20**(8): 887-900.

Shirazi-Adl, A. (1994). "Nonlinear stress analysis of the whole lumbar spine in torsion--mechanics of facet articulation." J Biomech **27**(3): 289-299.

Simmons, E. D. (2001). "Surgical treatment of patients with lumbar spinal stenosis with associated scoliosis." Clin Orthop Relat Res(384): 45-53.

Smit, T. H., M. S. van Tunen, A. J. van der Veen, I. Kingma and J. H. van Dieen (2011). "Quantifying intervertebral disc mechanics: a new definition of the neutral zone." BMC Musculoskelet Disord **12**: 38.

Spenciner, D., D. Greene, J. Paiva, M. Palumbo and J. Crisco (2006). "The multidirectional bending properties of the human lumbar intervertebral disc." Spine J **6**(3): 248-257.

Stokes, I. A., C. McBride, D. D. Aronsson and P. J. Roughley (2011). "Intervertebral disc changes with angulation, compression and reduced mobility simulating altered mechanical environment in scoliosis." European Spine Journal **20**(10): 1735-1744.

Stokes, I. A., C. A. McBride and D. D. Aronsson (2008). "Intervertebral disc changes in an animal model representing altered mechanics in scoliosis." Stud Health Technol Inform **140**: 273-277.

Tawackoli, W., R. Marco and M. A. Liebschner (2004). "The effect of compressive axial preload on the flexibility of the thoracolumbar spine." Spine (Phila Pa 1976) **29**(9): 988-993.

Thompson, R. E., T. M. Barker and M. J. Pearcy (2003). "Defining the Neutral Zone of sheep intervertebral joints during dynamic motions: an in vitro study." Clin Biomech (Bristol, Avon) **18**(2): 89-98.

Veldhuizen, A. G. and P. J. Scholten (1987). "Kinematics of the scoliotic spine as related to the normal spine." Spine (Phila Pa 1976) **12**(9): 852-858.

Waters, R. and J. Morris (1973). "An in vitro study of normal and scoliotic interspinous ligaments." Journal of biomechanics **6**(4): 343-348.

Weiss, H. R. and D. Goodall (2008). "Rate of complications in scoliosis surgery - a systematic review of the Pub Med literature." Scoliosis **3**: 9.

Wilke, H. J., K. Wenger and L. Claes (1998). "Testing criteria for spinal implants: recommendations for the standardization of in vitro stability testing of spinal implants." Eur Spine J **7**(2): 148-154.

Wilke, H. J., S. Wolf, L. E. Claes, M. Arand and A. Wiesend (1995). "Stability increase of the lumbar spine with different muscle groups. A biomechanical in vitro study." Spine (Phila Pa 1976) **20**(2): 192-198.

Zander, T., A. Rohlmann and G. Bergmann (2004). "Influence of ligament stiffness on the mechanical behavior of a functional spinal unit." Journal of biomechanics **37**(7): 1107-1111.

Zirbel, S. A., D. K. Stolworthy, L. L. Howell and A. E. Bowden (2013). "Intervertebral disc degeneration alters lumbar spine segmental stiffness in all modes of loading under a compressive follower load." The Spine Journal **13**(9): 1134-1147.